
CHAPTER 2

PASSIVE NORMALLY CLOSED MICRO CHECK-VALVES

2.1 Overview

Normally closed (NC) micro check-valve is used to stop liquid flow when liquid pressure difference across the membrane is lower than the designed cracking pressure. As shown in Figure 2-1, when the applied pressure P is lower than the designed cracking pressure, P_c , the NC check-valve is closed, and vice versa. Generally the cracking pressure can be introduced electrically such as electromagnetic force, mechanically such as MEMS springs, or other physical approaches such as stiction force. Passive check-valves usually use mechanical approaches to reduce complexity and thus no controlling circuit is needed. To mechanically implement controllable cracking pressures onto the NC micro check-valves, many different types of pre-stress technique have been developed, such as cantilever type, diaphragm type, and bivalvular type, etc. [105]. These NC check-valves use deformation of covering materials geometrically designed to provide the desired controlling force based on the requirements of applications. The material selection would also depend on the application of the micro check-valves. For example, if high cracking pressure is necessary, materials with large Young's modulus are used to provide the required pre-stressed force. Moreover, if the device is for human body implantation use, the biocompatible material such as parylene-C is needed to

fabricate the device. However, parylene-C has lower Young's modulus than general stiff MEMS materials such as poly silicon or silicon nitride. Therefore, parylene-C is not appropriate to construct a high-cracking-pressure NC check-valve using traditional configuration and a new design needs to be explored.

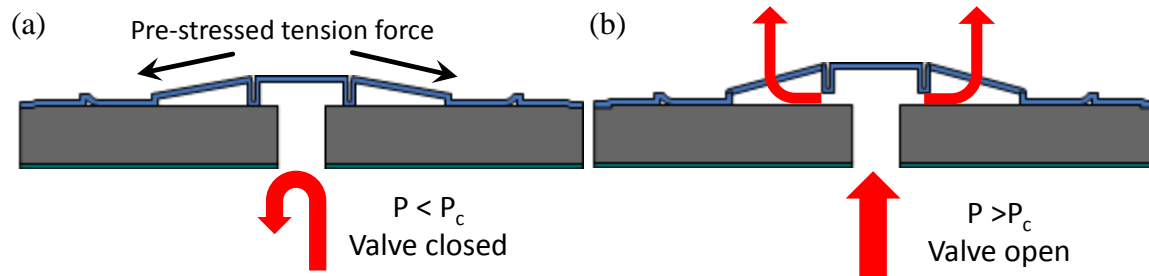


Figure 2-1: Concept of the normally closed (NC) check-valve: (a) The check-valve is closed when the applied pressure P is lower than the cracking pressure P_c ; (b) the check-valve is open when the applied pressure P is higher than the cracking pressure P_c .

Several different passive parylene-C micro check-valves have been developed in the past. For example, to generate a zero crack pressure NC check-valve, Wang developed a parylene-C micro check-valve with twist-up tethers to reduce membrane-induced flow resistance to a negligible level in 1999 [106]. On the other hand, to have a NC check-valve with a certain level of cracking pressure, Wang also developed in 2000 another type of NC micro check-valve with which a sealing plate is center-anchored by vacuum-collapse anchoring to achieve 20 kPa (2.9 Psi) of cracking pressure [107]. Xie developed another type of ideal NC micro check-valves with simpler check-valve structure than Wang's [108]. Xie's check-valve has nearly zero cracking pressure using the self-assembled monolayer (SAM) coating gold, which was found by the authors capable of reducing the adhesion of parylene-C and the silicon substrate so as to achieve the zero cracking pressure.

Among all the parylene-C NC check-valves mentioned above, only one check-valve is designed to be capable of providing the necessary cracking pressure, which is still limited in a certain low pressure range due to parylene-C's Young's low modulus of 3-4 GPa. This would restrict the NC check-valve to be used in high pressure applications. In addition, although the gas permeability of the parylene-C has been found to be very small, e.g., oxygen permeability of parylene-C is $2.8 \text{ cm}^3 \cdot \text{mm} \cdot \text{m}^2 \cdot \text{day}^{-1} \cdot \text{atm}^{-1}$ [100], the parylene-C vacuum-collapse anchoring can still be in vein after a long time of usage as the gas can still permeate through the parylene-C film into the cavity.

In this chapter, the theoretical flow-rate of micro check-valves and the amount of the necessary pre-stress force are first investigated. Then a simple passive NC check-valve structure is proposed and developed to be a standard MEMS NC check-valves paradigm. NC check-valves with different level of cracking pressure are designed, fabricated and characterized to cover a broad pressure range of applications. With very similar structures, all of them consume no power, and are made of parylene-C to guarantee the biocompatibility. The cracking pressure is obtained by stretching the parylene-C using residual tensile stress introduced after thermal quenching (high pressure applications), or by stiction and pop-up structure (low pressure applications). Although with only 3-4 GPa of the parylene-C Young's modulus, these pre-stress approaches can still overcome the inefficiency by providing larger strain and thus make high cracking-pressure parylene NC check-valve possible.

2.2 Theoretical Analysis of NC Micro Check-Valves

2.2.1 Thin-film-flow theory of the check-valve

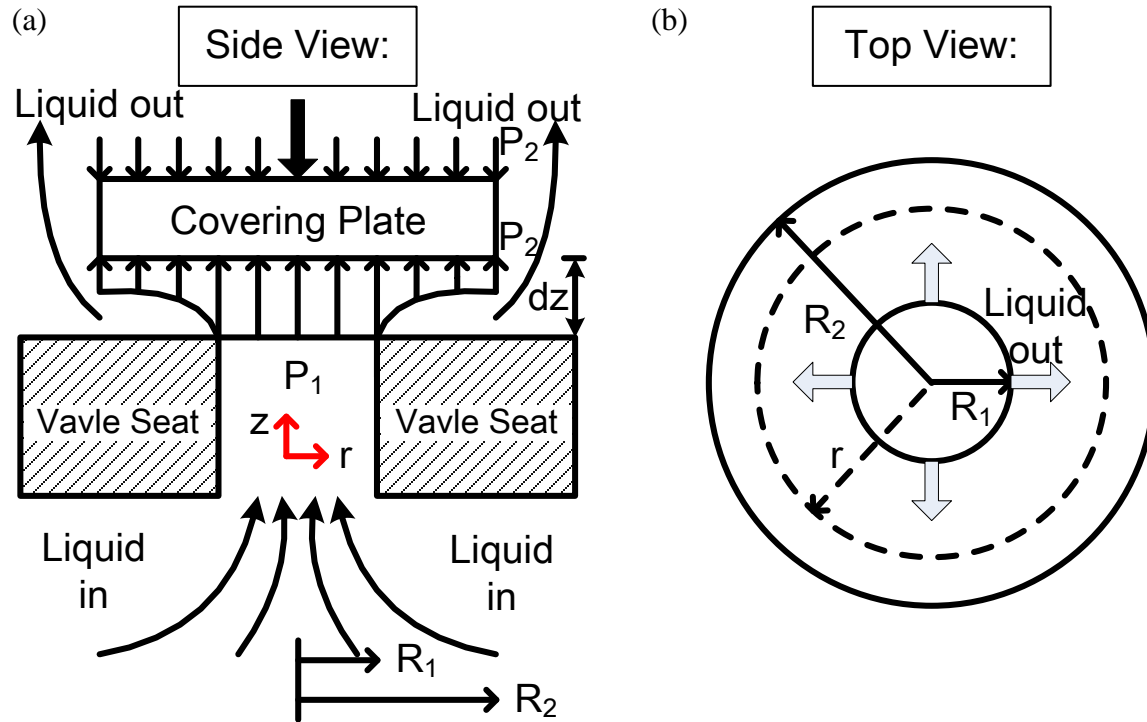


Figure 2-2: Check-valve model for unsteady flow analysis: (a) side view, and (b) top view

A simplified check-valve configuration is shown in Figure 2-2. The check-valve is normally closed owing to a pre-stressed downward force. The covering plate opens when the forwarding force of the liquid becomes higher than the downward force. After the covering plate pops open, the liquid flows in between the covering plate and the valve seat, forming a very thin capillary flow layer. The flow-rate equation in such case has not been fully developed so that the problem needs to take into account some unsteady flow effects. Several assumption are made to simplified the calculations: (1) The flow is incompressible, and asymmetrical; (2) the upstream pressure, P_1 , is uniformly applied on

the covering plate within the range of $r \leq R_l$, the radius of the opening, and so is the downstream pressure, P_2 , which is the pre-stressed downward force; (3) the weight of the liquid is negligible; (4) the opening gap, g , is much smaller than R_l .

At low Reynolds numbers found in this thin film flow, the Navier-Stokes equation can be reduced into the Reynolds equations of hydrodynamic lubrication as follows [109]:

$$\frac{\partial p}{\partial z} = 0, \text{ and } \frac{\partial p}{\partial r} = \mu \frac{\partial^2 u_r}{\partial z^2}, \quad (2-1)$$

where p is the pressure in the liquid film, μ is the dynamic viscosity and u_r is the radial velocity component. From the integration of eqn. (2-1), we can get radial velocity as:

$$u_r(z) = \frac{1}{2\mu} \frac{dp}{dr} z(z - g). \quad (2-2)$$

Therefore, the volume flow-rate can be represented as:

$$Q(r) = \int_0^g u_r(z) 2\pi r dz = -\frac{\pi r}{6\mu} \frac{dp}{dr} g^3. \quad (2-3)$$

By conservation of mass, the volume flow-rate can be also shown as:

$$Q(r) = Q(R_1) - \pi(r^2 - R_1^2) \frac{dg}{dt}, \quad (2-4)$$

where $\pi(r^2 - R_1^2) \frac{dg}{dt}$ represents the volume increase within R_l and r . Equal eqns. (2-3)

and (2-4), yields

$$r \frac{dp}{dr} = \frac{6\mu}{g^3} \frac{dg}{dt} (r^2 - R_1^2) + R_1 \left(\frac{dp}{dr} \right) \Big|_{r=R_1}. \quad (2-5)$$

Let $\frac{r}{R_1} = \lambda$ and $\frac{R_2}{R_1} = M$, and integrate equation (2-5) with respect to λ , then yields

$$p = \frac{3\mu}{g^3} \frac{dg}{dt} R_1^2 (\lambda^2 - 2\ln\lambda) + \ln\lambda \left(\frac{dp}{d\lambda} \right) \Big|_{\lambda=1} + C. \quad (2-6)$$

To solve the constant C and $\left(\frac{dp}{d\lambda} \right) \Big|_{\lambda=1}$, substitute the boundary conditions with $p=P_1$ at $\lambda=1$ and $p=P_2$ at $\lambda=M$ and we can get:

$$C = p_1 - \frac{3\mu}{g^3} \frac{dg}{dt} R_1^2, \quad (2-7)$$

and

$$\left(\frac{dp}{d\lambda} \right) \Big|_{\lambda=1} = \frac{1}{\ln M} \left[p_2 - p_1 + \frac{3\mu}{g^3} \frac{dg}{dt} R_1^2 (1 - M^2 + 2\ln M) \right]. \quad (2-8)$$

Substitute eqns. (2-7) and (2-8) into (2-6) and yields

$$p = p_2 + (p_1 - p_2) \left(1 - \frac{\ln\lambda}{\ln M} \right) + \frac{3\mu}{g^3} \frac{dg}{dt} R_1^2 \left[\lambda^2 - 1 + \frac{\ln\lambda}{\ln M} (1 - M^2) \right], \quad (2-9)$$

and hence the volume flow-rate of eqn.(2-3) becomes

$$Q(r) = (p_1 - p_2) \frac{\pi}{6\mu \ln M} - \frac{\pi r}{2} \frac{dg}{dt} R_1^2 \left(\frac{2r}{R_1^2} + \frac{1 - M^2}{r \ln M} \right). \quad (2-10)$$

The total force that the liquid applied on the covering plate can be expressed as:

$$\begin{aligned} F_{Total} &= (p_1 - p_2) \pi R_1^2 + F_{plate} = (p_1 - p_2) \pi R_1^2 + \int_1^M p 2\pi R_1^2 \lambda d\lambda \\ &= \left[(p_1 - p_2) \pi R_1^2 \left(\frac{M^2 - 1}{2 \ln M} \right) \right] \\ &\quad + \frac{\mu}{g^3} \frac{dg}{dt} \frac{3\pi}{2} R_1^4 \left[1 - M^4 + \frac{1 - 2M^2 + M^4}{\ln M} \right] \\ &= F_{steady} + F_{unsteady}, \end{aligned} \quad (2-11)$$

where F_{steady} represents the applied force in steady state flow due to the pressure difference, $P_1 - P_2$, while $F_{unsteady}$ represents the unsteady state condition. The second term

becomes zero if the covering plate's gap is fixed, i.e., $\frac{dg}{dt} = 0$, or $R_1=R_2$, or the dynamic viscosity, μ , is zero.

2.2.2 Calculation of the necessary pre-stress force

The liquid starts to flow when the upstream force is equivalent or higher than the downstream force. The force balance at this moment can be used to find the necessary pre-stress tensile stress and can be mathematically represented as:

$$p_1\pi R_1^2 \geq p_2\pi R_2^2, \quad (2-12)$$

or

$$p_1 \geq M^2 p_2 = p_c, \quad (2-13)$$

where p_c is defined as the cracking pressure of the check-valve. Assume the tensile stress of the slanted tethers is σ_t , the tethers' number, thickness, width, and angle are n , t , w , and θ , respectively, then the required tensile stress can be derived as

$$\sigma_t = \frac{\pi R_1^2}{twn\sin\theta} p_c. \quad (2-14)$$

As the tensile stress is generated by annealing the check-valve in high temperature T_1 and quenched to room temperature T_r , σ_t can also be represented as:

$$\sigma_t = E_p \alpha (T_1 - T_r), \quad (2-15)$$

where E_p and α are the Young's modulus and the thermal coefficient of expansion of parylene-C, respectively. The annealing temperature can be determined by eqn. (2-15).

2.3 Pre-Stressed Slanted Tether Micro Check-Valves

2.3.1 Slanted tether NC check-valve configuration

A simple NC check-valve structure schematic is proposed and shown in Figure 2-3. The check-valve is composed of single layer of parylene-C with several slanted tethers. The slanted tethers are reinforced to provide the necessary downward force which introduces the designed cracking pressure of the NC check-valve. With this simple slanted tether NC check-valve design, the downward force can be controlled by several parameters: the number of the slanted tethers, the sloping angle of the slanted tethers (θ), the geometry of the slanted tethers (the width and the thickness), and also the residual stress of the slanted tethers which can be controlled by annealing temperatures. The structure design greatly simplifies Chen's multi-layer parylene-C micromachining process into single-layer parylene-C deposition.

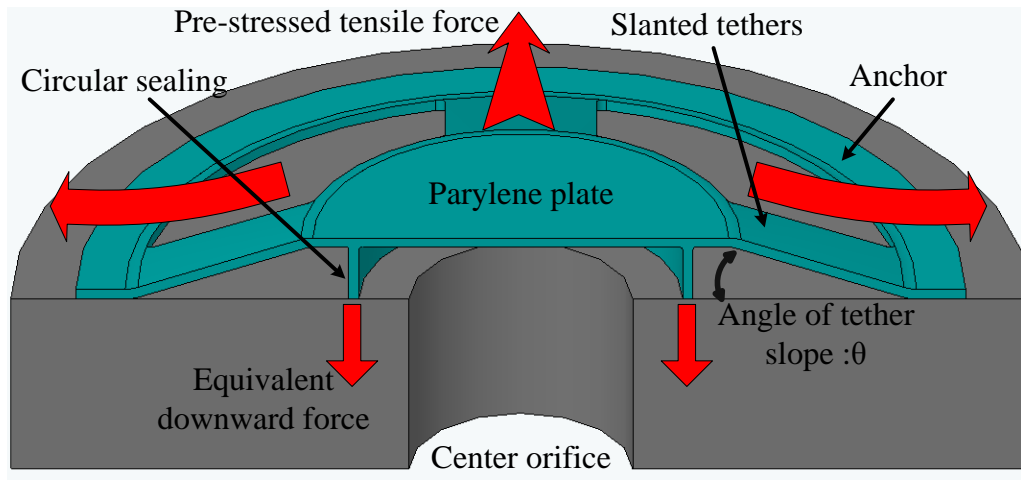


Figure 2-3: Schematic of cracking-pressure-controlled parylene-C check-valve using the residual tensile stress in parylene-C after thermal annealing

2.3.2 Thermal annealing pre-stressed NC check-valves

With the structure designed as in Figure 2-3, the slanted tethers are thermally annealed at predetermined temperature after the sacrificial photoresist is released and quenched down to room temperature afterwards. Since the residual tensile stress of the thermally annealed parylene-C can be as high as 34 MPa at 250°C [110], this approach allows the parylene-C tethers to provide a high downward force while it does not require any post-fabrication manual manipulation.

In order to utilize the residual tensile stress in parylene-C after thermal annealing, we need to make parylene-C tethers slanted with an angle, θ . After the check-valves are processed with sacrificial photoresist releasing, they are annealed at a desired temperature and then quenched quickly to room temperature. Because the thermal expansion coefficient of parylene-C is much bigger than that of the silicon substrate, this process generates a residual tensile stress in the slanted tethers. This residual tensile stress then provides a net downward sealing force on the parylene-C NC check-valve's covering plate against the silicon orifice. The final cracking pressure can be mathematically represented as:

$$P_c = \frac{t \times w \times n \times \sigma_t \times \sin\theta}{\pi r^2}, \quad (2-16)$$

where P_c is the cracking pressure of the valve; t is the thickness of the parylene-C; w is the width of the tethers; n is the number of the tethers; σ_t is the residual stress of thermally annealed parylene-C; and r is the radius of the parylene-C covering plate. With the thermally annealing residual tensile stress at 250°C as 34 MPa, the cracking pressure of this check-valve can be achieved as high as several psi even for a small size check-valve.

2.3.3 Sloped photoresist

2.3.3.1 One-time-exposure gray-scale photo-mask

The technique of using one-time-exposure gray-scale lithography to create the sloped photoresist [111–117] is introduced in this section. The one-time-exposure gray-scale lithography technique was originally invented to fabricate the diffractive optical elements (DOE) [113]. Due to its capability of generating sloped photoresist, the technique has also been used as the etching mask to create the sloped shape MEMS devices [112, 117]. In this work, the technique is used to make sloped sacrificial photoresist in the check-valve fabrication process.

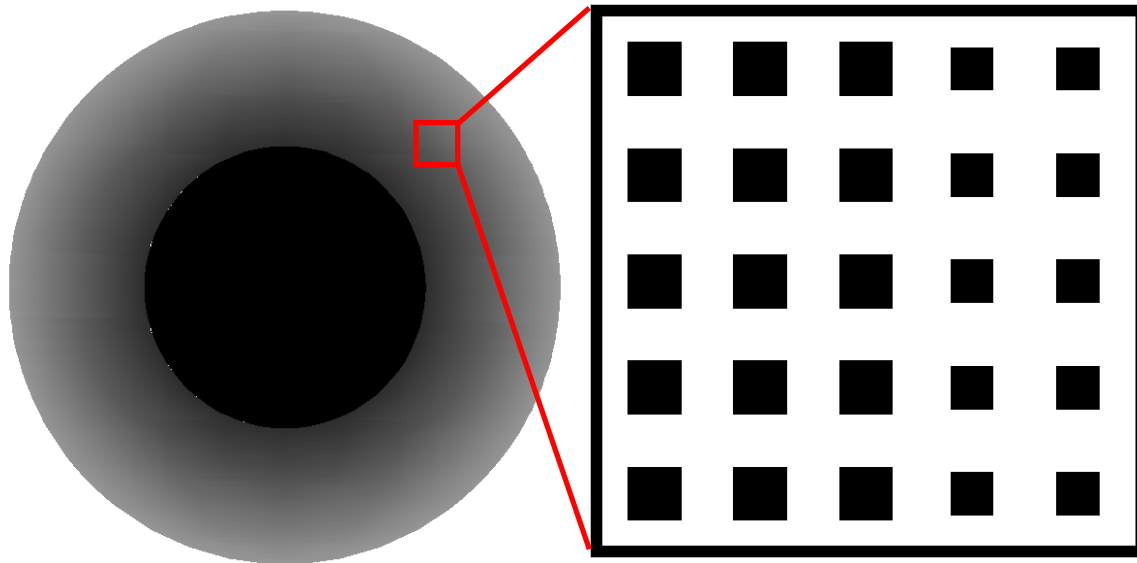


Figure 2-4: A closer view of designed gray-scale photo-mask for the creation of sloped photoresist. The right pattern magnifies part of the pixel structure of the ring.

Such a typical photo-mask is shown in Figure 2-4. To make photoresist partially exposed, an array of small dark squares with pitch, P , smaller than the diffraction limit of

the UV exposure system, P_c , are designed onto the photo-mask. Dark squares with pitch smaller than the diffraction limit can actually make the first order diffraction light blocked by the numerical aperture of the exposure system, making the light transmittance of the photo-mask proportional to the coverage area of these dark squares [117].

The maximum allowable square pitch size which will not get resolved by the optical system can be expressed as:

$$P \leq P_c = \frac{1}{1 + \sigma} \times \frac{\lambda}{NA}, \quad (2-17)$$

where σ is the coherence factor of the optical system, λ is the UV wavelength, which is 436 nm in our optical exposure system. NA is the numerical aperture of the optical exposure system. According to the specification of our exposure stepper, the diffraction limit is about 1 μm . In the transmittance design, “pulse width modulation” approach is used, in which a constant square pitch with various dark square sizes as shown in Figure 2-4. With the 10:1 optical image reduction, we can have dark squares $> 10 \mu\text{m}$ on our photo-mask. Therefore, it is relatively low-cost to perform the gray-scale-mask lithography using the regular commercially available transparency slides [115].

2.3.3.2 Linearization of the sloped sacrificial photoresist

It is well known that most photoresists have nonlinear response to UV light exposure. Therefore, a gray-scale photo-mask pattern with linear transmittance distribution will not give us a linear photoresist profile, as shown in Figure 2-5 (a). A mathematical model is adopted here to characterize and linearize our final photoresist profile [111]. In the model, the original total percentage of unexposed photoresist is normalized as 1, and the percentage of exposed photoresist is denoted as $E(t)$, which is generated after exposure to UV light within a period of time, t . It is further assumed that

the changing rate of exposed photoresist, $E(t)$, is proportional to the remaining unexposed photoresist, $1 - E(t)$, and the exposed light intensity I_0T , where I_0 is the stepper light intensity and T is the transmittance of the photo-mask. Therefore, the overall exposure system can be represented as an ordinary differential equation with the initial condition as follows,

$$E(0) = 0, \quad (2-18)$$

and

$$\frac{dE(t)}{dt} = \alpha[1 - E(t)]I_0T, \quad (2-19)$$

where α is the proportional constant. The constant is an optical property of the photoresist's sensitivity to UV light. The solution of eqns. (2-18) and (2-19) can be obtained as

$$E(t) = 1 - \exp(-\alpha I_0 T t). \quad (2-20)$$

Therefore, to have a linear distribution of exposed photoresist, $E(t)$, we can use eqn. (2-20) to design the corresponding transmittance distribution on the photo-mask. Figure 2-5 (b) shows the scanning result of the characterized and then linearized photoresist profile.

Figure 2-5 (b), the gray-scale photo-mask is composed of 16 levels with increasing transmittance from left to the right of the sloping area with each level translating into a photoresist height proportional to $\exp(-\alpha I_0 t)$. In order to create a true linear slope, a test photoresist strip was first fabricated for characterization. Then, the transmittance of each ring is adjusted according to the resulted photoresist height from

the test strip. It was shown in literature that larger $\alpha I_0 t$ produces more reliable results [111]. In our case, I_0 is measured as 200–250 mw/cm^2 in the stepper, which is one order of magnitude higher than the published literature. With t taken as 4 seconds, our exposure energy is within the right regime suggested in the literature.

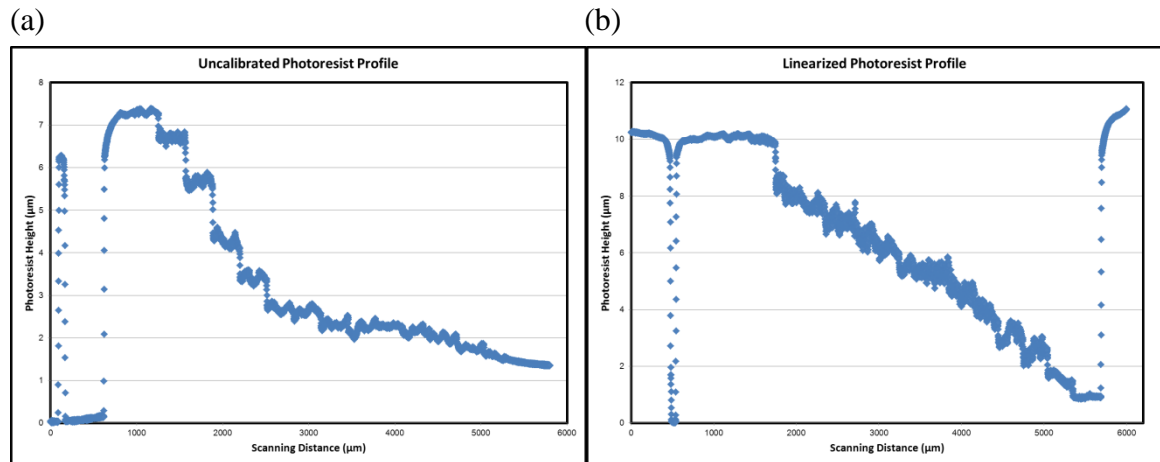


Figure 2-5: One-time-exposure gray-scale sacrificial photoresist profile: (a) before linearization, and (b) after linearization

2.3.4 Fabrication

Fabrication procedures are outlined in Figure 2-6. The process started with thermally growing silicon dioxide on both sides of double-side-polished wafers. After a back side oxide patterning, DRIE was used to etch the backside orifices with 100 μm in diameter and also the releasing trench, until a thin silicon membrane of 50 μm was left. A 100 μm deep thin circular trench was etched on the front side followed by coating and patterning parylene-C as an anchor to help hold the parylene-C check-valve in place during valve operation. A 10 μm photoresist AZ4620 was then coated on the front side and patterned using a gray-scale photo-mask. A two-step exposure technique with different exposure times was utilized to make the center photoresist to have variable

heights serving the mold of the valve sealing ring. After 10 μm of parylene-C coating and patterning, the through holes and trenches were completed by DRIE etching. The sacrificial photoresist was then removed by acetone and IPA.

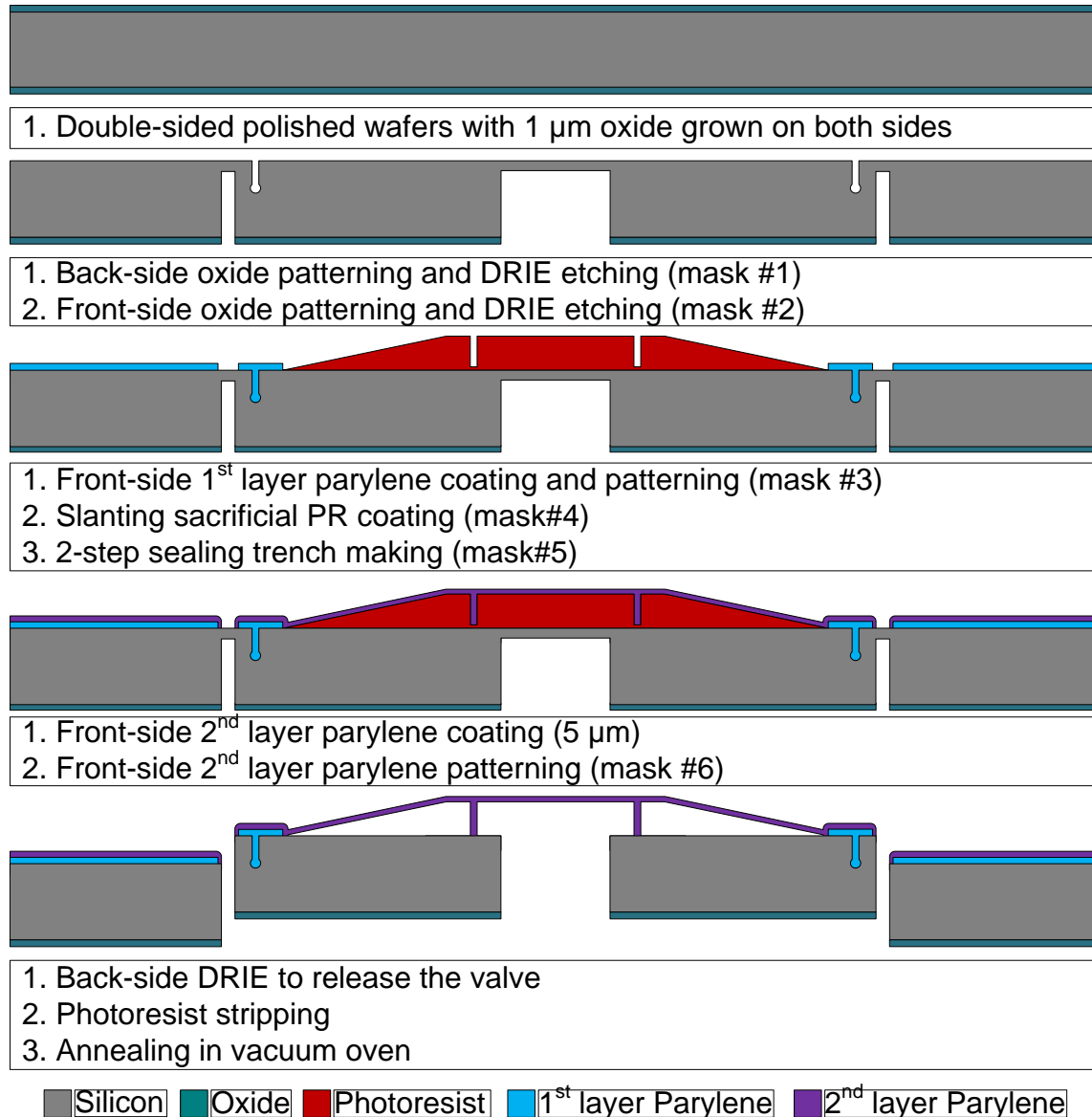


Figure 2-6: Fabrication procedures. Slanted sacrificial photoresist is achieved using a one-time-exposure gray-scale photo-mask photolithography approach.

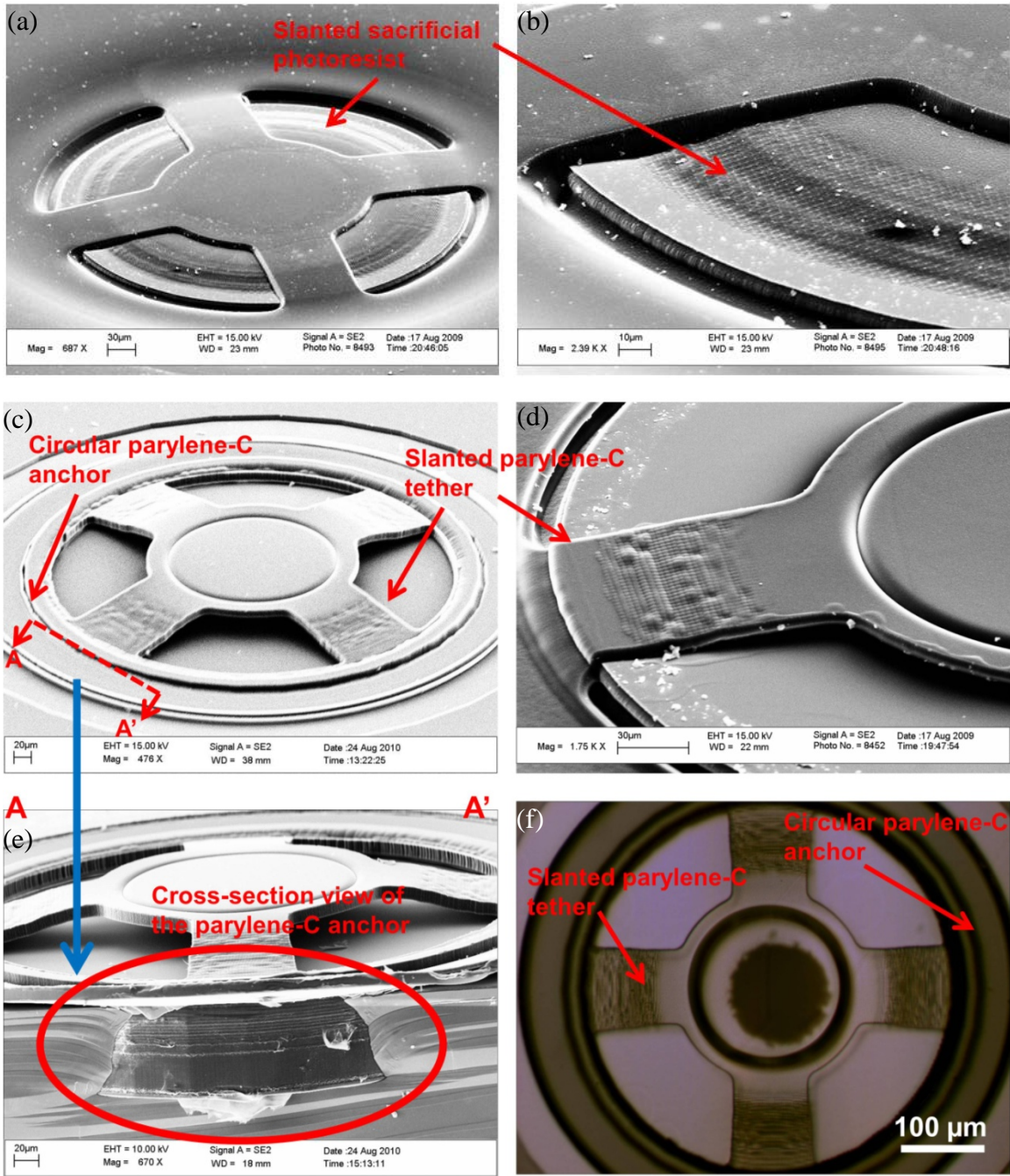


Figure 2-7: SEM pictures of fabricated check-valves: (a) check-valves before photoresist removal, (b) a closer view of a tether and the sloped photoresist, (c) check-valves after photoresist removal, (d) a closer view of a tether after photoresist removal, (e) the cross-sectional view of the parylene-C anchor, and (d) micrograph of the top view of the check-valve

SEM images of fabricated devices before and after photoresist stripping are shown in Figure 2-6 (a) to (e). Figures 2-6 (a) and (b) illustrate the successful creation of the slanted sacrificial photoresist profile by the one-time-exposure gray-scale lithography. Figures 2-6 (c) and (d) demonstrate the resulted linearly slanted parylene-C tethers after removing the photoresist. Figure 2-6 (e) shows the cross sectional view of the successful parylene-C anchor. Figure 2-6 (f) is the micrograph of the top view of the check-valve.

2.3.5 Device testing and discussion

After sacrificial photoresist was stripped by acetone and IPA, a thermal annealing of the NC check-valves was performed. Different temperatures were used to create different residual tensile stresses. The testing setup is shown in Figure 2-8. Water was chosen as the testing fluid. Working fluid flowed into a customized jig with specially designed channels conducting water to fluidic ports of the tested check-valves. Pressure was conducted to the check-valves through the backside orifices and flow-rate was recorded by measuring the marching speed of the testing fluid front inside the testing tubes.

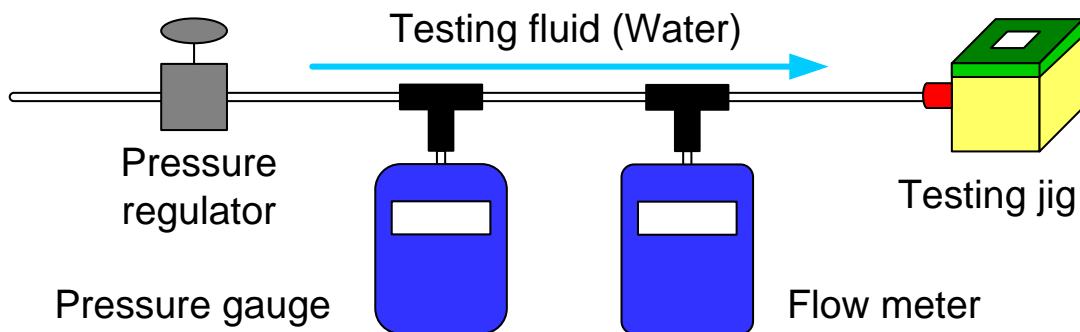


Figure 2-8: Testing setup for MEMS micro check-valves

Two cracking pressure controlling factors were considered and tested: parylene-C tether width and the annealing temperature. To study the influence of the parylene-C tether width, check-valves with 3 different tether widths (50 μm , 70 μm , 100 μm) were all annealed at 100°C for 1 hour and then quenched to room temperature to generate the necessary residual tensile stress. The pre-annealed check-valves were characterized by the proposed testing setup and the cracking pressures were measured to be 0.3 psi, 1.5 psi, and 2.9 psi, respectively as shown in Figure 2-9. It is shown that the check-valve's cracking pressure increases as the tethers widen. This agrees with our expectation because increased width means increased pre-stressed force.

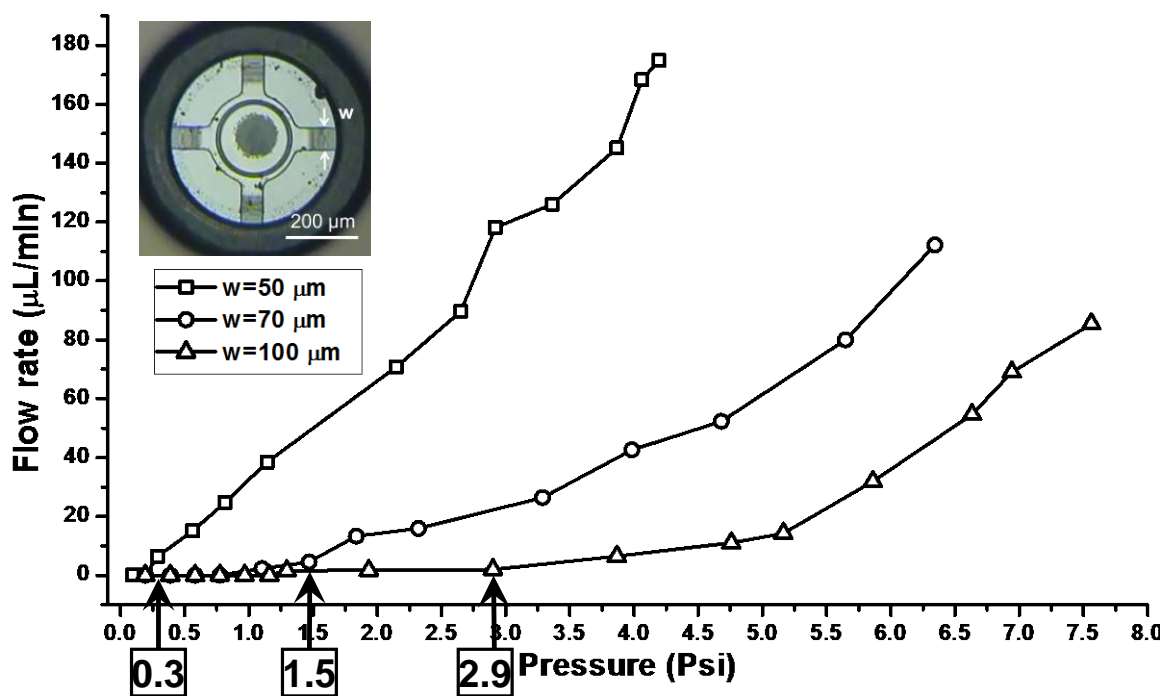


Figure 2-9: Parylene-C tether width effect of the characterization results of thermally pre-stressed slanted tether micro check-valves: different tether widths but with the same annealing temperature at 100°C

To study different annealing temperature effect, check-valves with 50 μm -wide-tether were annealed at 100°C and 140°C, quenched to room temperature, and then characterized. The process of annealing check-valves at 140°C was performed in vacuum to prevent the oxidation of parylene-C. The flow-rates are shown and compared in Figure 2-10. The cracking pressures were obtained as 0.3 psi and 1.3 psi for 100°C and 140°C, respectively. It is found that the cracking pressure increased as the annealing temperature increases. This is attributed to the increased residual tensile stress of parylene-C after annealed at higher temperatures.

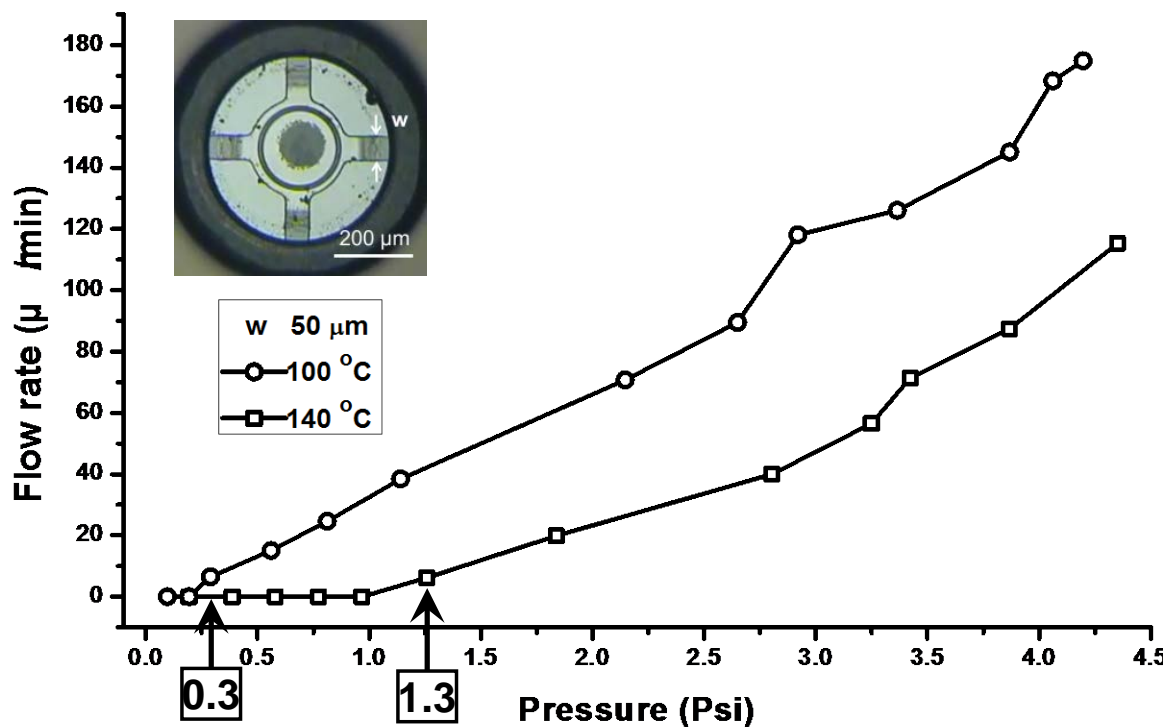


Figure 2-10: Temperature effect of the characterization results of thermally pre-stressed slanted tether micro check-valves: different annealing temperatures but with the same tether widths of 50 μm

To summarize, the cracking pressures of NC check-valves consistently increase with the increasing tether width and the annealing temperature. However, experimental data also showed that the cracking pressure could deviate from the theoretical value. This is likely because the flexibility of the parylene-C covering plate which cannot provide a strong fixed boundary condition. Therefore, the induced thermal stress cannot be as high as calculated. In addition, it is also found that, even at the room temperature, the cracking pressure tends to decrease at the early measuring stage after annealing. This is due to the stress relaxation of the parylene-C tethers right after annealing. The phenomenon of stress relaxation of parylene-C will be discussed more in detail in Section 5.8.3.

2.4 Integration of Slanted Tether Check-Valves for High-Pressure Applications

The thermally pre-stressed slanted-tether micro check-valves has been proved to be capable of delivering cracking pressures as high as 2.3 psi in Section 2.3. The check-valves' tethers are reinforced by quenching check-valves to room temperature after the stress-relaxation annealing process to induce high residual tensile stress in the tethers. However, even though the cracking pressure of this slanted tether check-valve can be adjusted by annealing at different temperature, the maximum cracking pressure achievable with a single check-valve is still limited by the bonding strength between parylene-C and silicon in the anchor region, and also the ultimate tensile strength of the parylene-C tethers.

In this section, multiple slanted tether check-valves are integrated in series to achieve even higher cracking pressures. In a series construction, each slanted tether

check-valve could be modeled as a diode, where pressure and flow-rate are analogous to voltage and current respectively. Using this model, multiple check-valves can be easily analyzed and connected in series to achieve a larger total pressure drop even though the pressure drop across each check-valve is smaller. This situation is similar to using a series connection of multiple diodes to achieve a higher total voltage drop.

2.4.1 Electrical-equivalent diode model

As shown in Figure 2-2, the volume flow-rate, Q , at $r = R_2$ equals the final exit flow-rate of the check-valve. Q can be calculated and rearranged from eqn. (2-10) as

$$Q(r)|_{r=R_2} = (p_1 - p_2) \frac{\pi}{6\mu \ln M} - \frac{dg}{dt} \left(\pi R_2^2 + \frac{\pi}{2} \frac{R_1^2 - R_2^2}{\ln M} \right). \quad (2-21)$$

Therefore, in order to successfully generate the flow-rate, the applying pressure of the liquid p_1 needs to be higher than the cracking pressure, p_c , shown in eqn. (2-13) with the flow-rate presented eqn. (2-21). The whole system can be equivalently modeled as a diode shown in Figure 2-11 with cut-in voltage as p_c . The flow-rate in eqn. (2-21) can be modeled as the electrical current after the cut-in voltage.

2.4.2 Multiple check-valve integration

The check-valves were first annealed at 140°C and quenched to room temperature to introduce the residual tensile stress in tethers. To assemble the device, each check-valve was first inserted into a thin glass capillary tube, whose inner diameter is 530 μm, and sealed with epoxy as shown in Figure 2-12 (a). These individual assemblies were then characterized to obtain their cracking pressure and flow profile. Photoresist was used to seal the gap between the assembly and the testing tube so that the assembly can be released for later integration, as shown in Figure 2-13 (b). Afterwards, each pair of

assemblies were coupled together with a wider capillary tube (inner diameter of $660\ \mu\text{m}$) to form an assembly of multiple check-valves, as shown in Figure 2-12 (b), then sealed with epoxy, and tested as shown in Figure 2-13 (c).

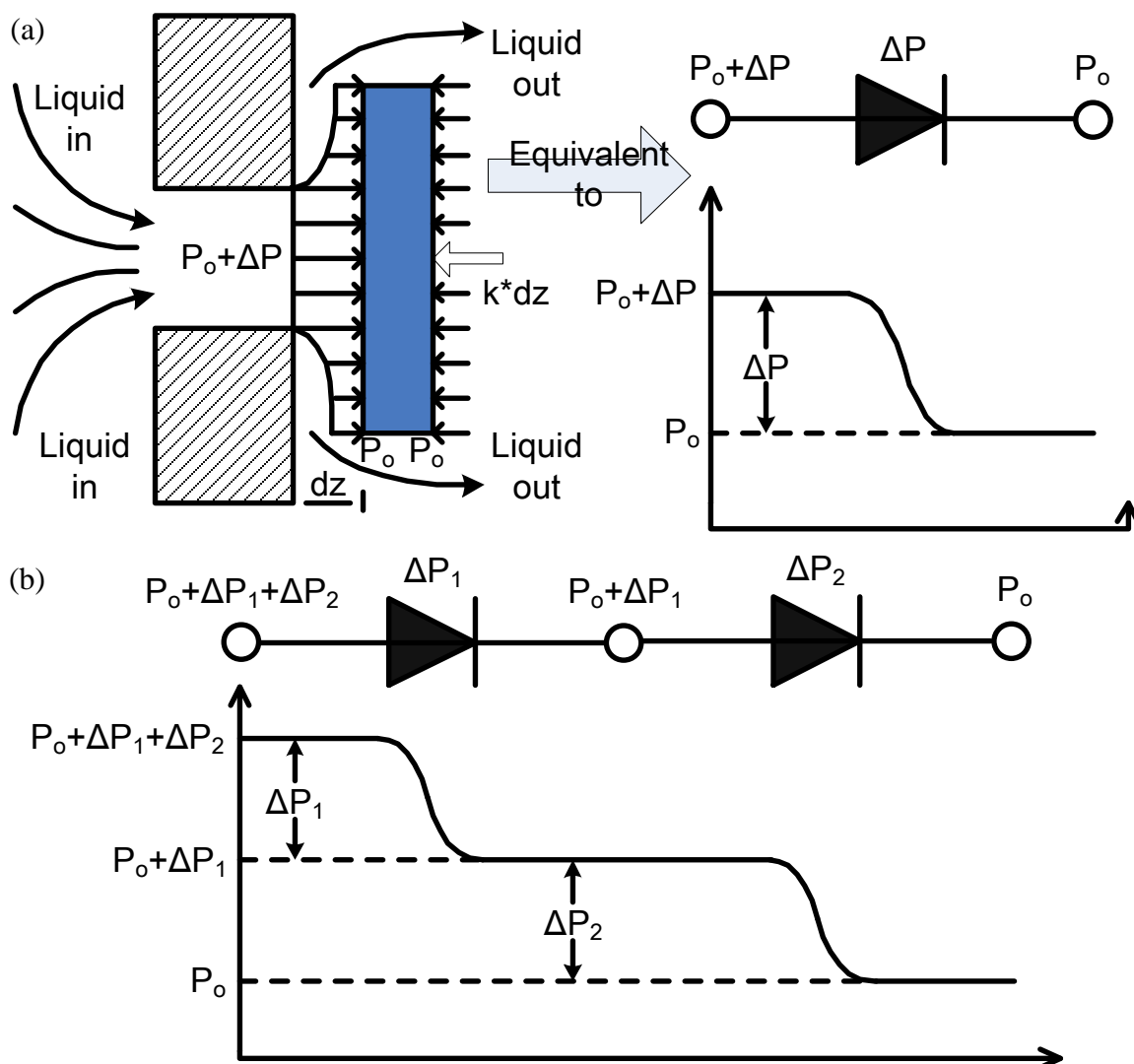


Figure 2-11: Equivalent electrical circuit component model of check-valves: (a) one-diode model of one check-valve. k and dz are the spring constant of the tethers and the covering plate displacement, respectively. (b) In-series diodes model of in-series check-valves

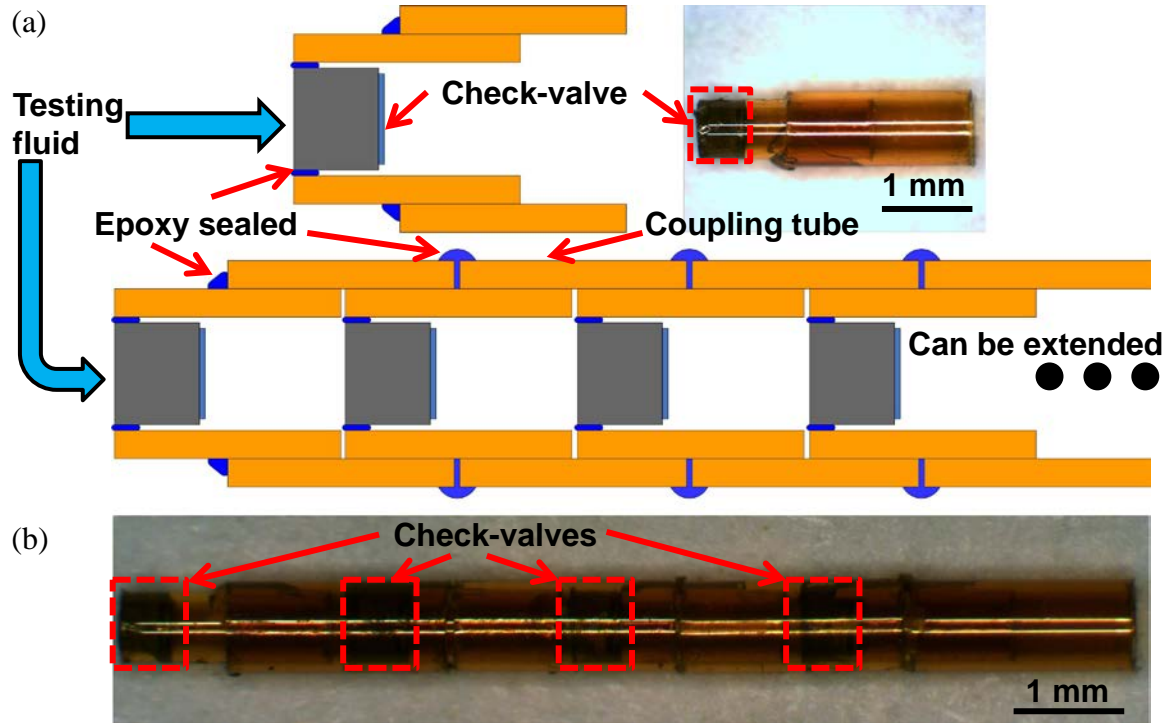


Figure 2-12: Valve packaging: (a) A single valve packaged in capillary tubes and (b) four individual modules integrated using coupling tubes

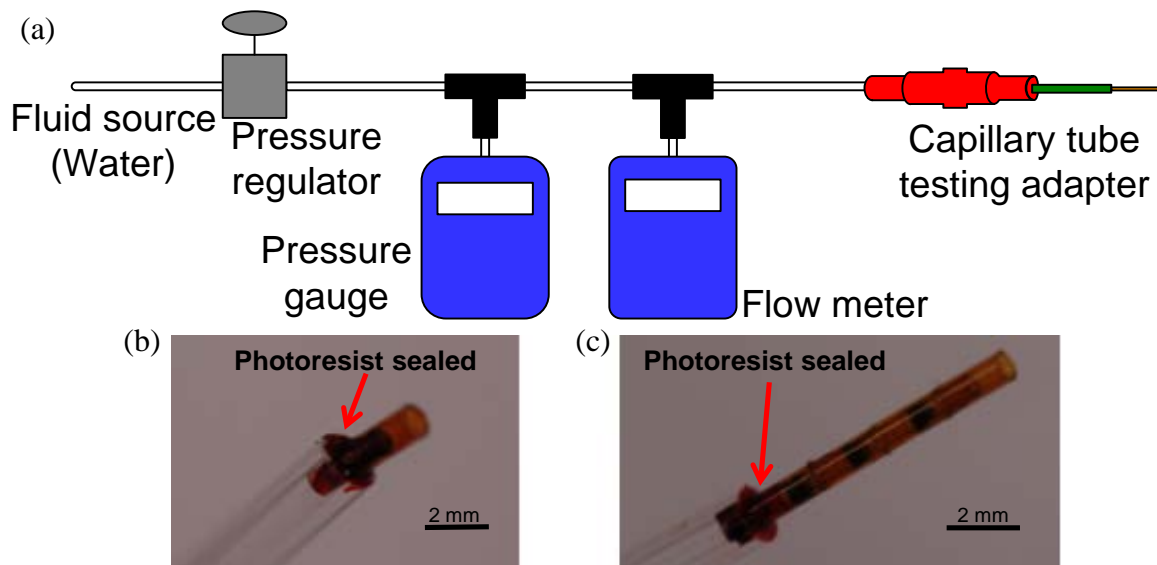


Figure 2-13: (a) Modified device testing setup, (b) the characterization of single valve, and (c) the characterization of four check-valves in series

2.4.3 Characterization results and discussion

The measured cracking pressures of each check-valve and the check-valve assembly are listed in Table 2-1. The flow profiles comparison between a single check-valve and a four-check-valve assembly is shown in Figure 2-14. The results show that the cracking pressure of a single valve falls between 0.42 psi and 0.49 and achieves 2.06 psi with four integrated check-valves. The parylene-C check-valves remain intact after many tests with inspection shown in Figure 2-14 (b). This proves the durability of the parylene-C anchors of the check-valve, which are to prevent de-bonding due to both the high tensile stress within the parylene-C layer after annealing process and the high pressure during the entire characterization process. The results verify the concept of integrating multiple slanted tether check-valves in series to create a high cracking pressure device for high-pressure microfluidic applications.

Table 2-1: Measured cracking pressures of four single check-valves and the assemblies of multiple check-valves

Single valve	1	2	3	4
Cracking pressure	0.49 psi	0.43 psi	0.47 psi	0.42 psi
Multiple valves	2 valves		3 valves	4 valves
Cracking pressure	1.01 psi		1.48 psi	2.06 psi

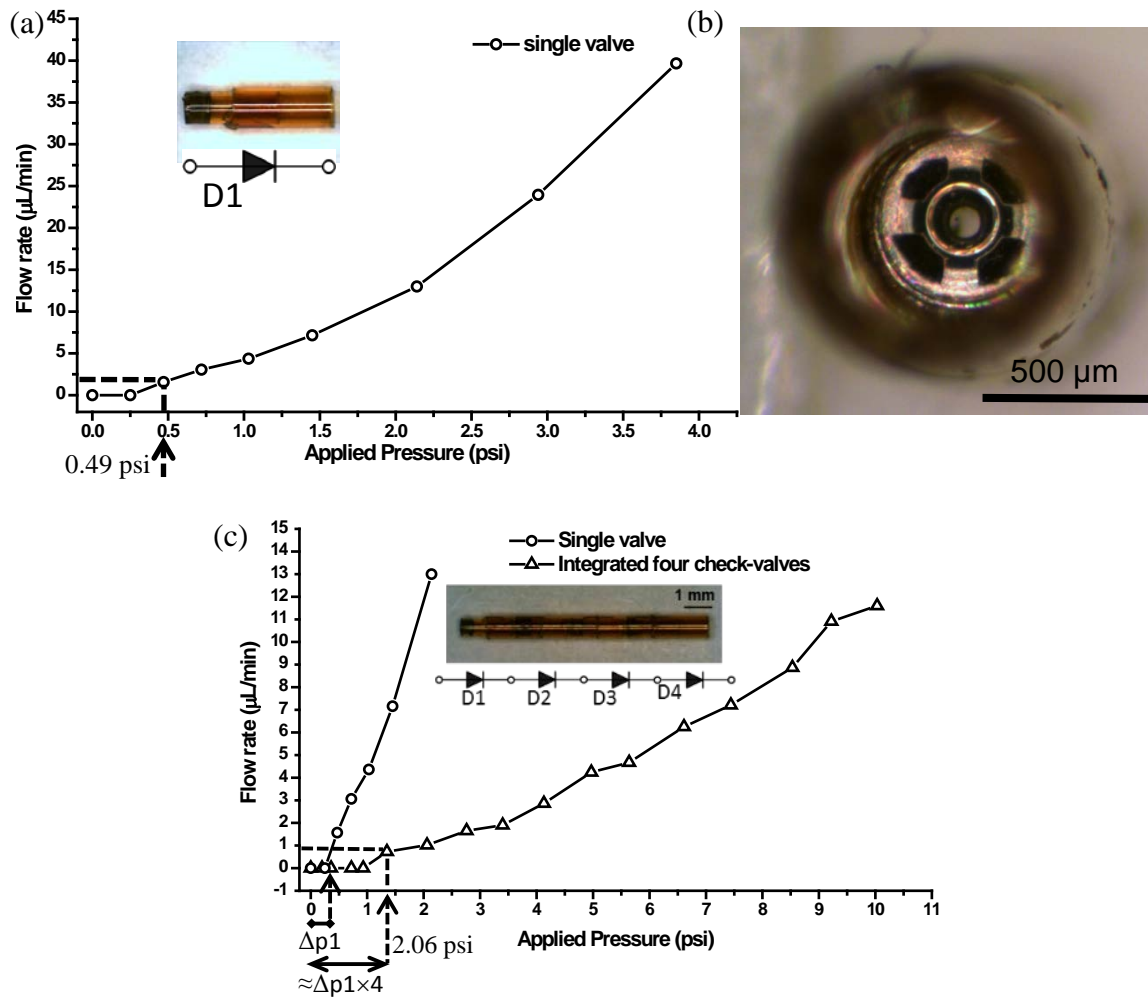


Figure 2-14: (a) Flow characteristics of a single valve, (b) micrograph of a check-valve in tube after testing, (c) flow characteristics of a four-check-valve assembly

2.5 Pop-Up Micro Check-Valve

The NC check-valves developed in Section 2.3 and the integrated multiple check-valves assembly in Section 2.4 have successfully demonstrated their capability of regulating pressure in a broad range (0.3 psi to several psi). However, it is found not simple enough to be integrated inside a channel so as to enable integrated microfluidics. In this section, a releasable all-parylene-C microfluidic device incorporating innovative

surface micro-machined NC pop-up check-valve is designed to regulate the cracking pressure of microfluidic flow. An undercut parylene-C foot is generated by first spin-coating a layer of LOR30B on silicon surface and then developed to create undercut after the first layer parylene-C film deposition and patterning. The cracking pressure is created by residual tensile stress built within the tethers introduced by post-fabrication pop-up process and can be enhanced by thermal annealing. This newly-designed micro check-valve can also be encapsulated within the all-parylene channel. The zigzag appearance along the channel edge makes it easy to anchor in any kind of implantation environments.

2.5.1 Pop-up micro check-valve device design

The design of the pop-up check-valve is shown in Figure 2-15. The structure requires an undercut beneath the first layer parylene-C, which is created by developing LOR30B, using the first parylene-C as the mask. The 2nd layer of parylene-C then fills into these undercuts during deposition and creates an interlocking structure between the two parylene-C layers and the covering plate which is made of the second layer of parylene-C. Before the check-valve's usage, the covering plate is popped up from the back side by flowing liquid through the through hole. Once popped, the covering plate will stay on top of the first layer parylene-C due to the undercut parylene-C foot and will no longer return to the original interlocked position. The popping first creates an amount of mechanical tensile stress within the tethers connecting the covering plate and valve's anchor because of the extension. The tethers can then be thermally pre-stressed with thermal tensile stress by annealing/quenching to further control the cracking pressure. The cracking pressure can still be predicted by eqn. (2-16). The proper length of the

undercut is determined to be 10 μm experimentally so that the covering plate can be popped up by injecting liquid into the back side through holes.

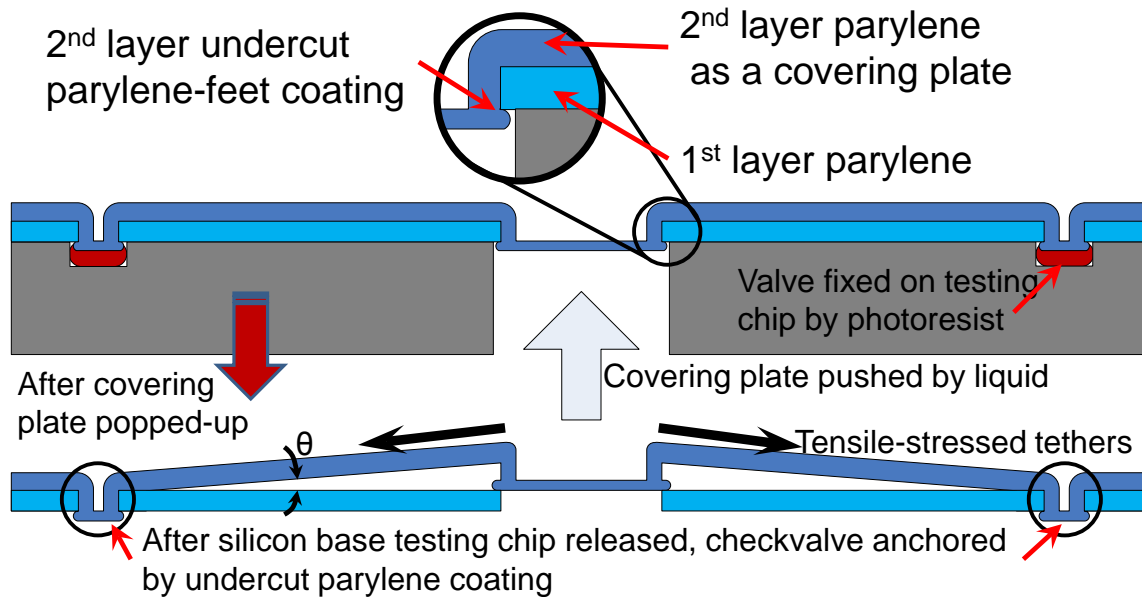


Figure 2-15: The configuration of a pop-up check-valve. A close-up of the undercut parylene-C foot is shown in the circular area.

2.5.2 Device fabrication

Both fabrication procedures of in-channel check-valves and testing chips were designed and are shown in Figure 2-16. The check-valve fabrication started with coating LOR30B on silicon wafers. A thin layer of aluminum was thermally evaporated onto LOR30B and then patterned to protect LOR30B from the possible hard baking during the following parylene-C layer plasma etching. The first layer of parylene-C was coated onto LOR30B and patterned. LOR30B undercut was developed after aluminum striping. The wafer was then coated with soap before the second layer of parylene-C deposition. After soap soaking on the parylene-C surface, the hydrophilic head of the soap was exposed

that changed the parylene-C surface to hydrophilic. This would benefit the popping process as the parylene-C would be easier to delaminate from the hydrophilic surface. The second layer of parylene-C was deposited, filling the undercut, and then patterned. A thick sacrificial layer of photoresist was coated, patterned and encapsulated with the third layer of protection parylene-C membrane. The whole device was released by acetone after patterning. On the other side of the parylene-C channel, an outlet port was fabricated using the same procedures as the check-valve, as shown in Figure 2-16 (a). The covering plate was etched away to make the through hole of the outlet port.

The testing chip fabrication started with double-side oxide wafers, with front side first patterned and etched by DRIE twice to create necessary cavities and then the back side DRIE followed to create through holes, as shown in Figure 2-16 (b).

The fabrication results are shown in Figure 2-17. Figure 2-17 (a) shows the successful undercut creation of LOR30B under the first layer of parylene-C; Figure 2-17 (b) is the micrograph of the check-valve after the second layer parylene-C patterned; Figure 2-17 (c) shows the micrograph of the top view of the outlet port after the second parylene-C patterned, and Figure 2-17 (d) demonstrates the final devices shown in 6 mm long. The zigzag features along the devices' sides facilitate the anchoring during the device implantation.

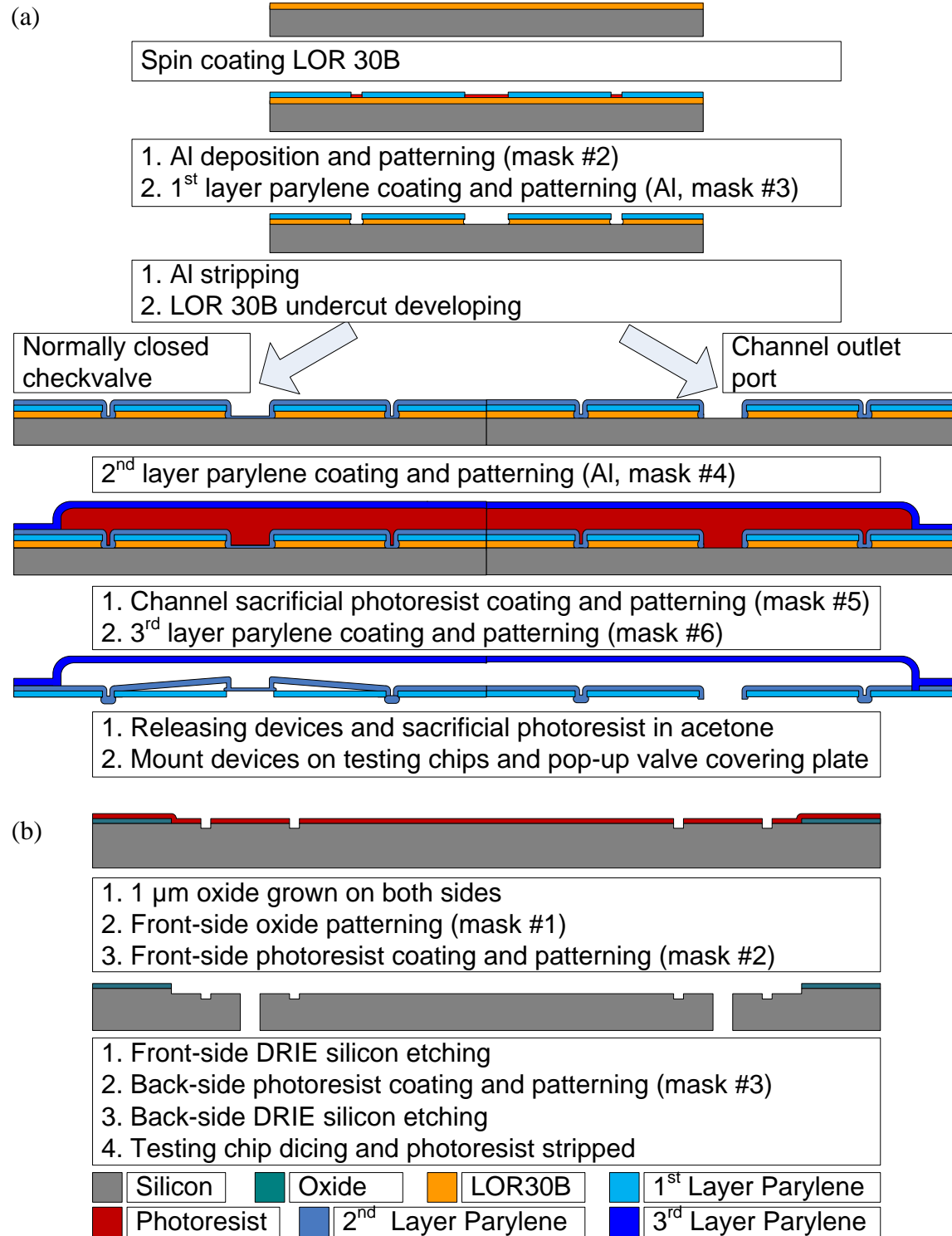


Figure 2-16: Fabrication procedures of (a) the pop-up micro check-valve, and (b) the testing chips

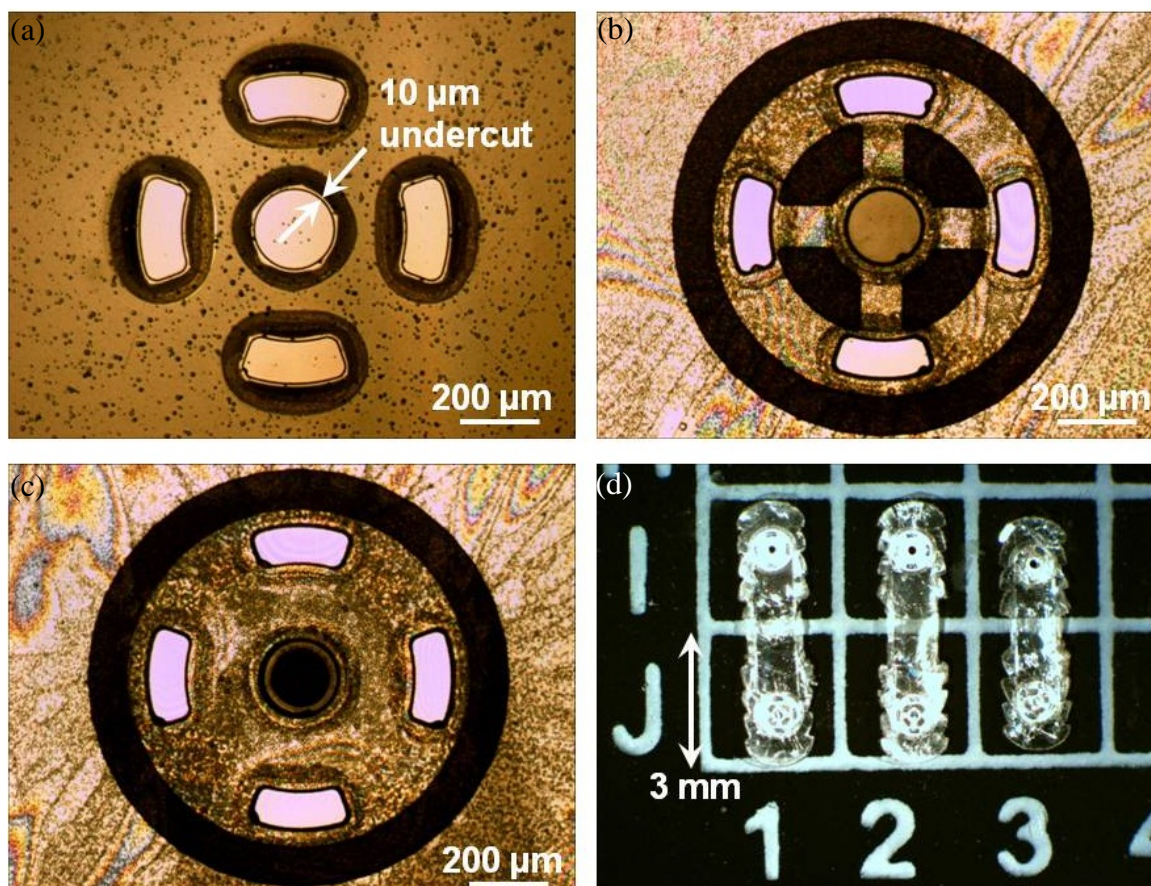


Figure 2-17: Micrograph of (a) 10 μm undercut of the LOR30B, (b) top view of the NC check-valve, (c) top view of the outlet orifice, and (d) final device appearance

Figure 2-18 shows a series of SEM pictures of the fabricated check-valves. Figure 2-18 (a) shows the backside view of the check-valve, presenting the successful undercut parylene-C-foot coating; Figure 2-18 (b) represents a close view of about 10 μm wide undercut coating; Figure 2-18 (c) is a top view of the check-valve before pop-up, and (d) is a close view of the tethers after pop-up. As shown in Figures 2-18 (a) and (b), four undercut parylene-C-foot not only work to anchor the check-valves onto the first layer parylene-C, but also behave as the posts preventing the device from stiction to the application surface.

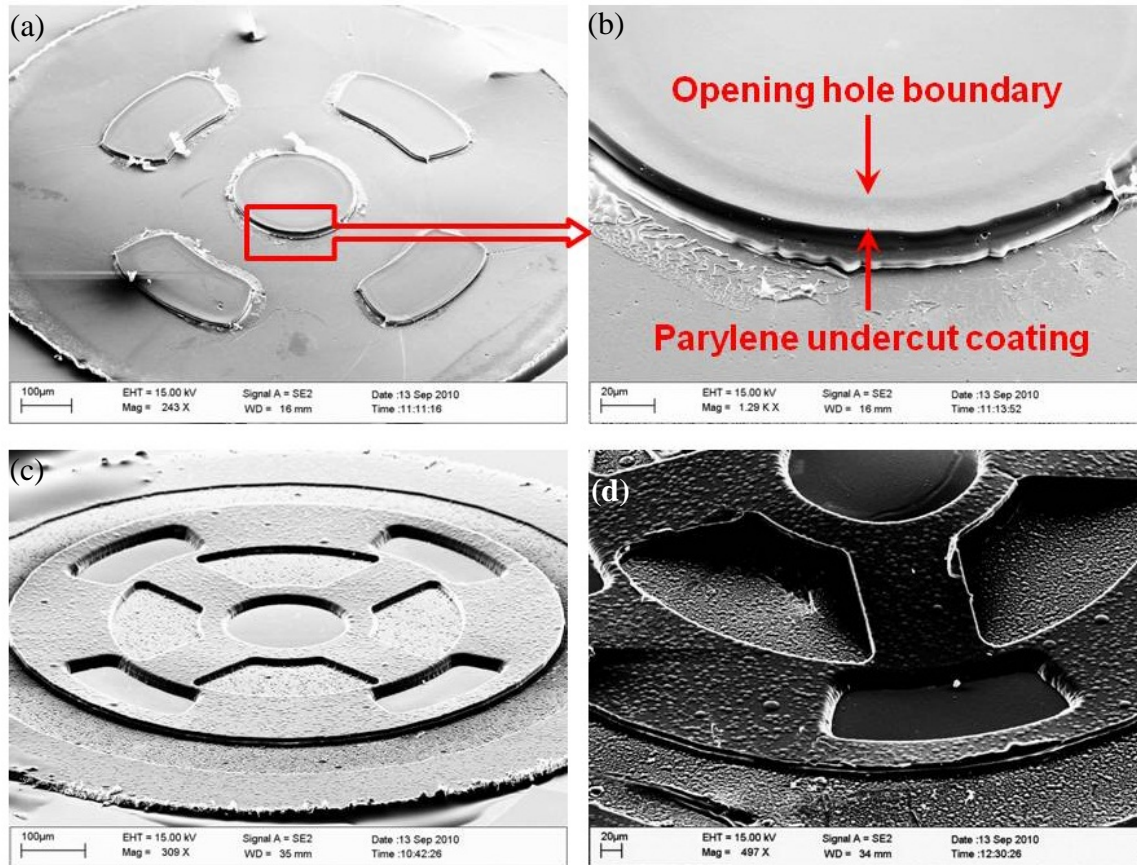


Figure 2-18: SEM pictures of (a) undercut parylene-C foot coating (back side view), (b) close view of undercut parylene-C foot coating, (d) normally closed check-valve, and (d) covering plate after pop-up

2.5.3 Device characterization setup

A complete testing chip is shown in Figure 2-20 (a). The size of the indentation on the testing chip is designed a bit larger than the device so that the through holes of the check-valves can be aligned with the holes of the testing chips. Circular trenches with the same width as check-valves' posts are fabricated to accommodate the posts so as to ensure the flatness of the check-valves and the complete sealing during the testing.

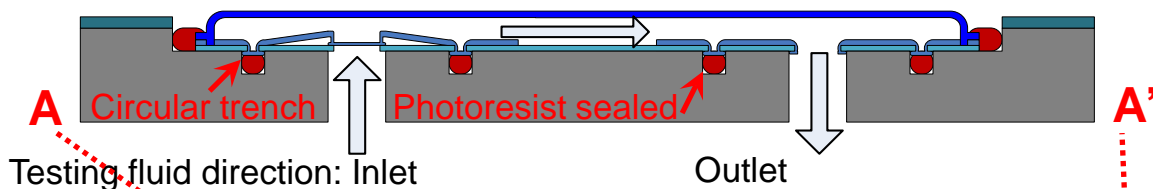


Figure 2-19: Cross section view of the testing chip with mounted in-channel check-valve

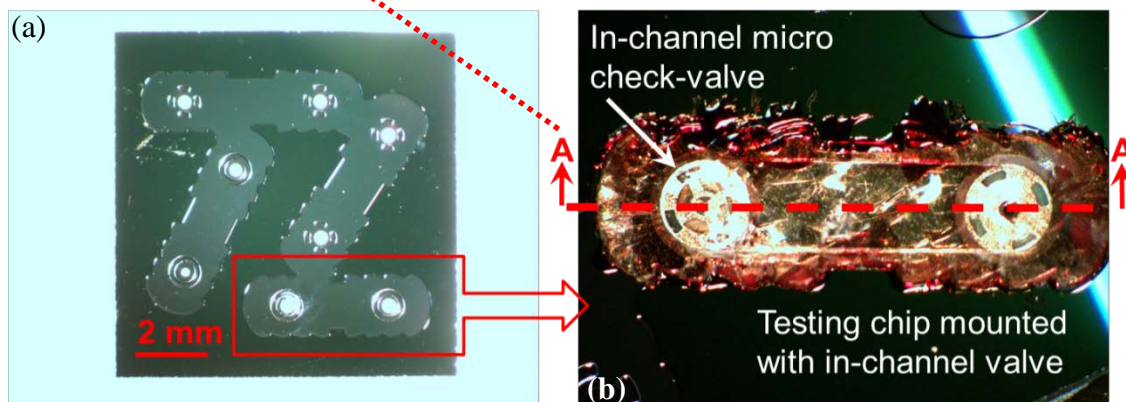


Figure 2-20: (a) Top view of the fabricated testing chip. (b) A close view of mounted device on top of the testing chip, sealed with dried photoresist

To test the in-channel check-valves, devices released from photoresist were first soaked in 5% HF solution. HF solution penetrates the top parylene-C layer into the boundary between two parylene-C layers and cleans the boundary. This makes it easier to separate the first and the second parylene-C layers during the popping-up. To enhance the check-valves' cracking pressure, devices were first annealed in high temperature in the oven to release all inherent residual stress, and then quenched to room temperature to build the necessary residual tensile stress. Rather than unpredictable residual stress, the stress achieved this way can be more controllable. Devices were then mounted onto the testing chip which was aligned and fixed on top of the testing jig as shown in Figure 2-20 (b). Photoresist was applied to seal and anchor the posts in the circular trench. The

surroundings of the device were also sealed by photoresist to ensure complete sealing. The testing setup shown in Figure 2-8 was used to characterize single check-valve. The check-valves were first popped up by pushing water into the back holes, and then microfluidically characterized. As shown in Figure 2-19, the testing liquid was sent into left NC check-valve. The liquid flew through the channel and exit to the right outlet port. The tested and qualified devices were then released in acetone to remove the photoresist for later implantation applications, as shown in Figure 2-17 (d)

2.5.4 Device characterization results

The popping process was filmed to observe its transition behavior. During the popping process, a syringe was used to inject the liquid into the through holes to gradually increase the applied pressure. When the applied pressure was higher the confining pressure of the interlock of the covering plate and the first layer parylene-C, the liquid burst out flowing. The applied pressure was released afterward, and the covering plate stayed on top of the first layer parylene-C due to the undercut parylene-C-foot. Figure 2-21 shows a sequence of pictures captured from the video: (a) shows the situation when applied pressure almost reached the confining pressure. Liquid is still covered by the covering plate; (b) demonstrates the time when applied pressure is just right over the confining pressure. The covering plate is suddenly popped over the confinement hole and liquid can be clearly seen to burst flowing out the NC check-valve; (c) shows the liquid over flooded right after the popping-up.

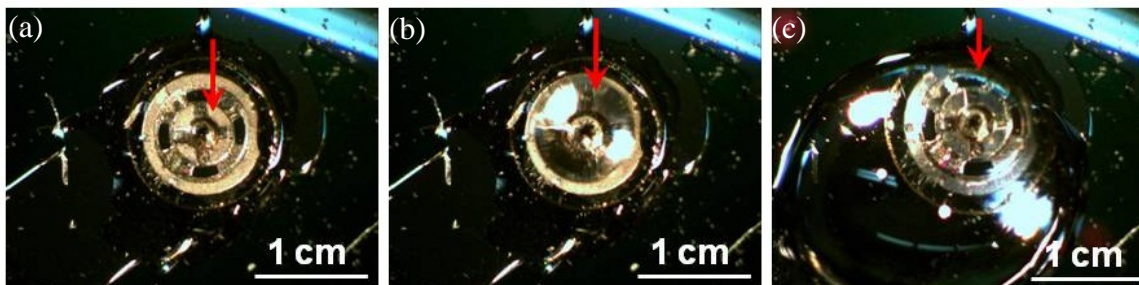


Figure 2-21: Captured pictures of normally closed pop-up check-valve during popping-up process (shown in arrow): (a) right before pop-up, (b) during pop-up, and (d) after pop-up. (Top parylene-C membrane is peeled off for clarity.)

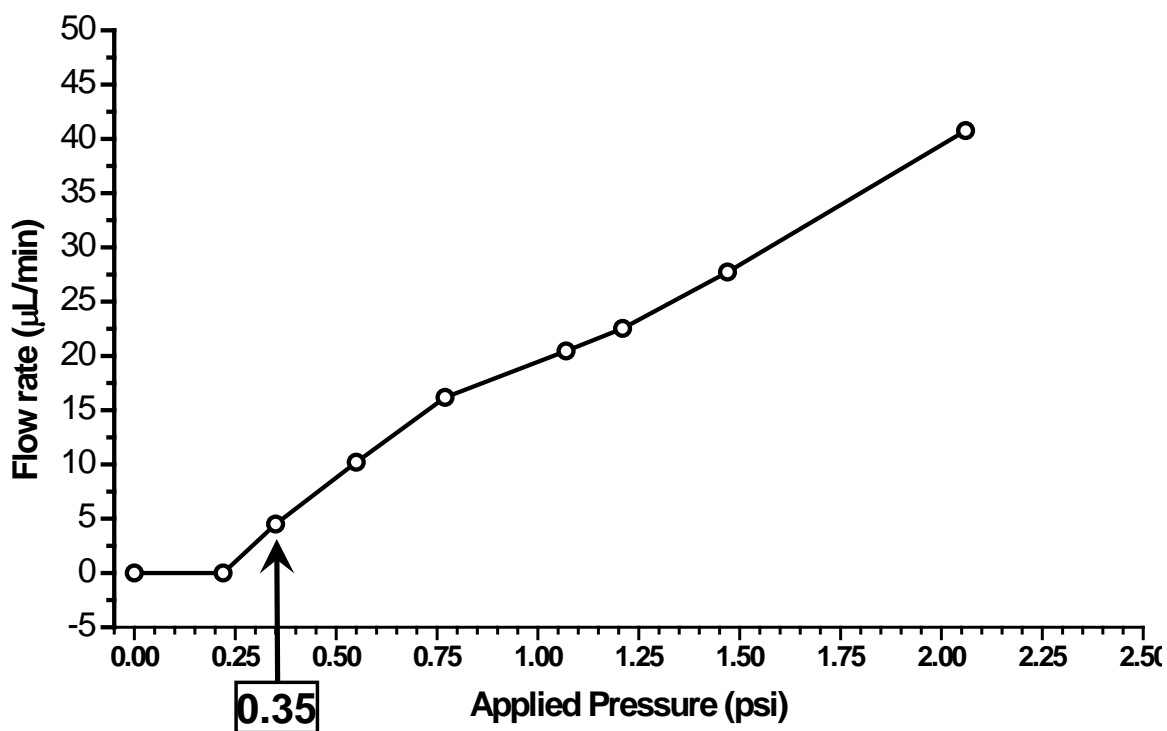


Figure 2-22: Testing result of the pop-up check-valve

After the popping process, a check-valve can be further annealed at 140°C to enhance the pre-stressed parylene-C tethers. Figure 2-22 shows the experimental result.

The cracking pressure of the check-valve is determined by the time when the liquid starts to flow. The flow characteristic is obtained with cracking pressure of 0.35 psi, verifying the feasibility of the pop-up check-valve. It is found that the flow-rate is similar to the check-valve shown in Figure 2-10, but with a lower cracking pressure in the pop-up check-valve. It is likely that the parylene-C base (the first layer parylene-C) is very easily damaged during the popping process. Besides, because the 10- μ m thick parylene-C base is still very flexible, the pre-stressed parylene-C tether would cause the parylene-C base to deform downward after the popping and thermal annealing. This causes smaller angle of the parylene-C tethers and therefore reduces the check-valve cracking pressure. Depositing thicker parylene-C base can solve the problem. In addition, coating a layer of metal would increase the Young's modulus of the parylene-C base and reduce the deformation amount caused by the pre-stressed parylene-C tethers.

2.6 Self-Stiction-Bonding Micro NC Check-Valves

2.6.1 Design concept of the self-stiction-bonding NC check-valve

Although the NC check-valve developed in Sections 2.3 to 2.5 has demonstrated the promising results of their capability of regulating the flow-rate, there still drawbacks exist in these NC check-valves. For the slanted check-valve utilizing the sloped sacrificial photoresist, it is more pricy to make the key gray-scale photo-mask. On the other hand, for the pop-up NC check-valve, the pop-up process might damage the parylene-C base easily and thus the yield rate is low. In this section, a NC check-valve is developed by manipulating the stiction phenomenon to create the necessary cracking pressure.

As shown in Figure 2-23, the self-stiction-bonding NC valve utilizes a stiction process that inevitably takes place after the drying process. According to theory [118–123], the parylene-C tether's length can be accurately designed for enough stiction while keeping the appropriate size of the micro NC check-valves. To generate enough stiction, the length of the parylene-C tether must be longer than the critical length of a cantilever beam which can be predicted as:

$$l_{crit} \geq \sqrt[4]{\frac{3}{16} \frac{Et^3 g^2}{\gamma_{la} \cos \theta_c}}, \quad (2-22)$$

where E , and t is the Young's modulus and the thickness of parylene-C, respectively. g is the gap spacing, γ_{la} is the surface tension of the liquid–air interface. θ_c is the contact angle between the drying liquid and the parylene-C.

This self-stiction effect facilitates spontaneous anchoring of the NC check-valve with predetermined cracking pressure by pre-stressing the center sealing part of the check-valve through straight tethers connecting to the anchoring part, as shown in Figure 2-23. The built-in stress of the parylene-C tethers comes from both the residual tensile stress remained after thermal annealing, and stretching due to stiction bonding. Cracking pressure can be controlled by many parameters as described in Section 2.3.1. Similar to the NC check-valve structure aforementioned, flow-rate is defined by the size of the opening orifice and the opening gap of the parylene-C membrane. Furthermore, few holes are designed on the stiction-bonding parts where epoxy can be used to further ensure bonding strength and to prevent parylene-C from de-lamination after repeated operations, as shown in Figure 2-25 (b).

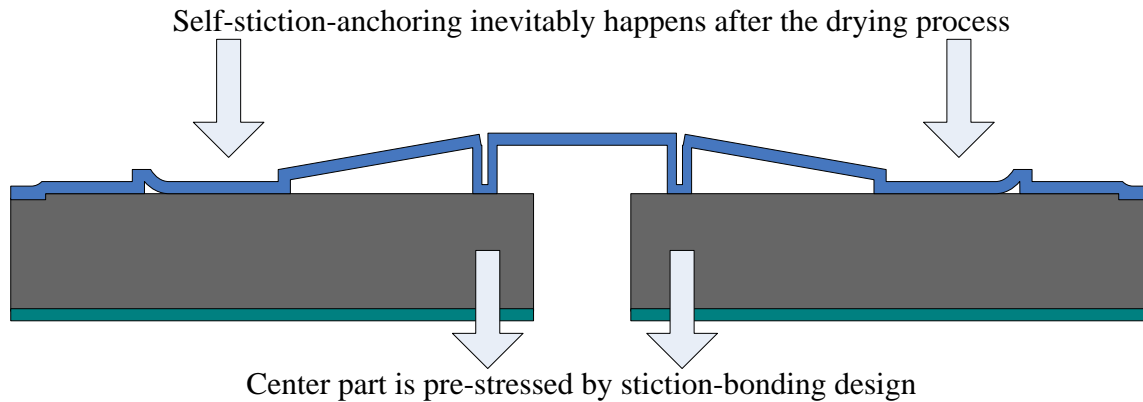


Figure 2-23: Schematics of the self-stiction-bonding NC check-valve

2.6.2 Fabrication of the self-stiction-bonding NC check-valve

The fabrication process started from growing thermal oxide on silicon wafer, as shown in Figure 2-24. Through-wafer holes and releasing trenches of the check-valves were etched using back-side DRIE until 50 μm silicon membranes was left. The circular boundary of the valve seats were defined here with diameter to be 500 μm , which can be fit into parylene-C protective tube's I.D. smoothly. XeF_2 was used to roughen the front side surface encircling the check-valve area to improve the adhesion between deposited parylene-C and the silicon valve seat. The three-step exposure lithography was performed to create three different heights of sacrificial photoresist for the NC check-valve. After parylene-C deposition, RIE was used to pattern the coated parylene-C and then through holes and the releasing trenches were opened by completely etching away the remaining silicon membrane by DRIE so as to strip the sacrificial photoresist with acetone and IPA.

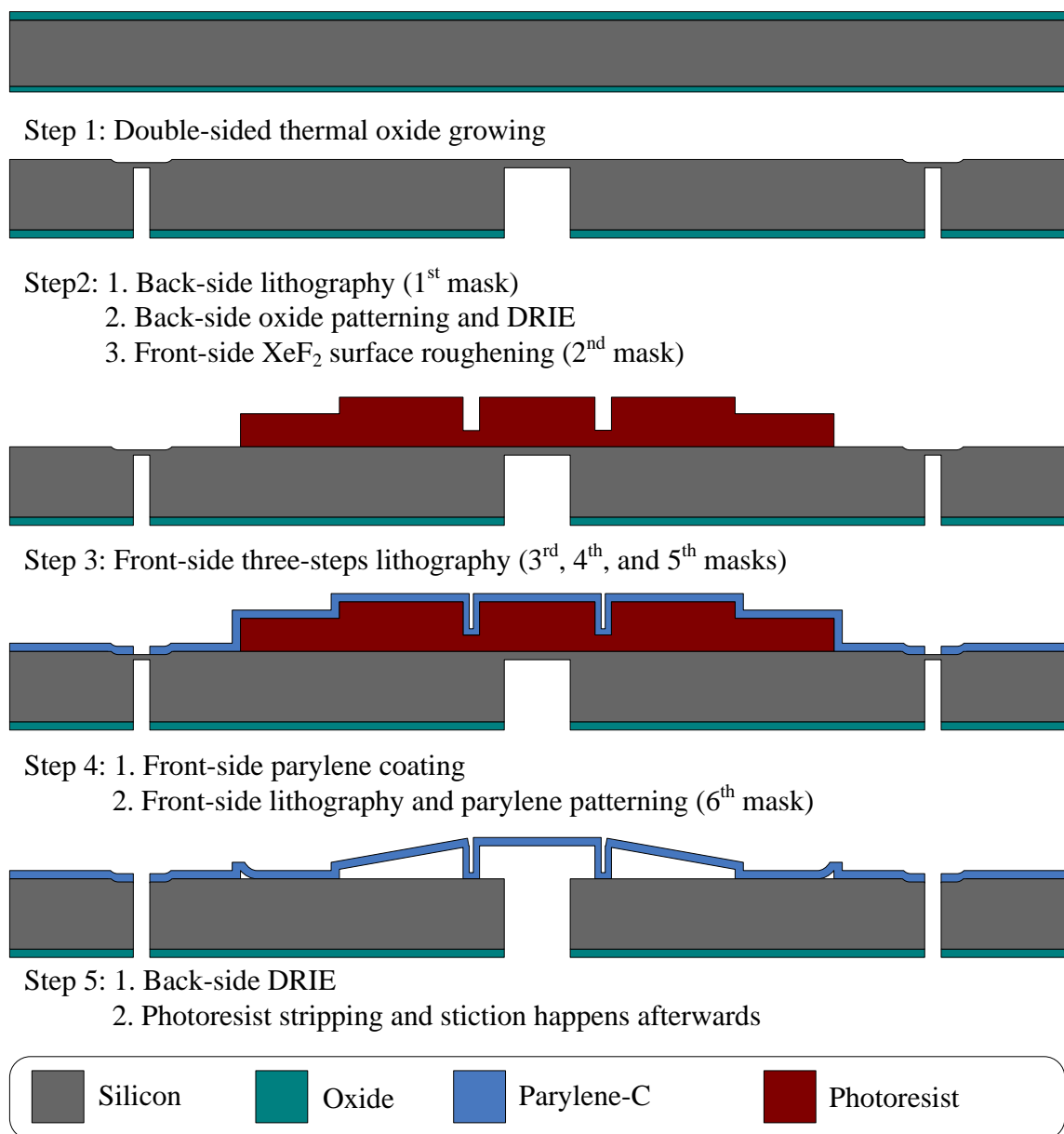


Figure 2-24: Fabrication procedures of the self-stiction-anchoring NC check-valve

Figures 2-25 (a) and (b) demonstrate the successful creation of the slanted parylene-C tethers through the self-stiction-bonding approach after the drying process. After photoresist stripping and air drying of the devices, stiction takes place on NC check-valves and the anchoring parts bonded onto silicon wafer surfaces, providing the necessary pre-stressed force through stretching the parylene-C tethers. The micrograph

of the fabrication result of the completed micro NC check-valve is illustrated in Figure 2-25 (c). To further enhance the bonding strength, tiny epoxy drops were then manually applied onto these NC check-valves' stiction-bonding parts to make sure the parylene-C won't de-laminate after several repeated operations, as shown in Figure 2-25 (d).

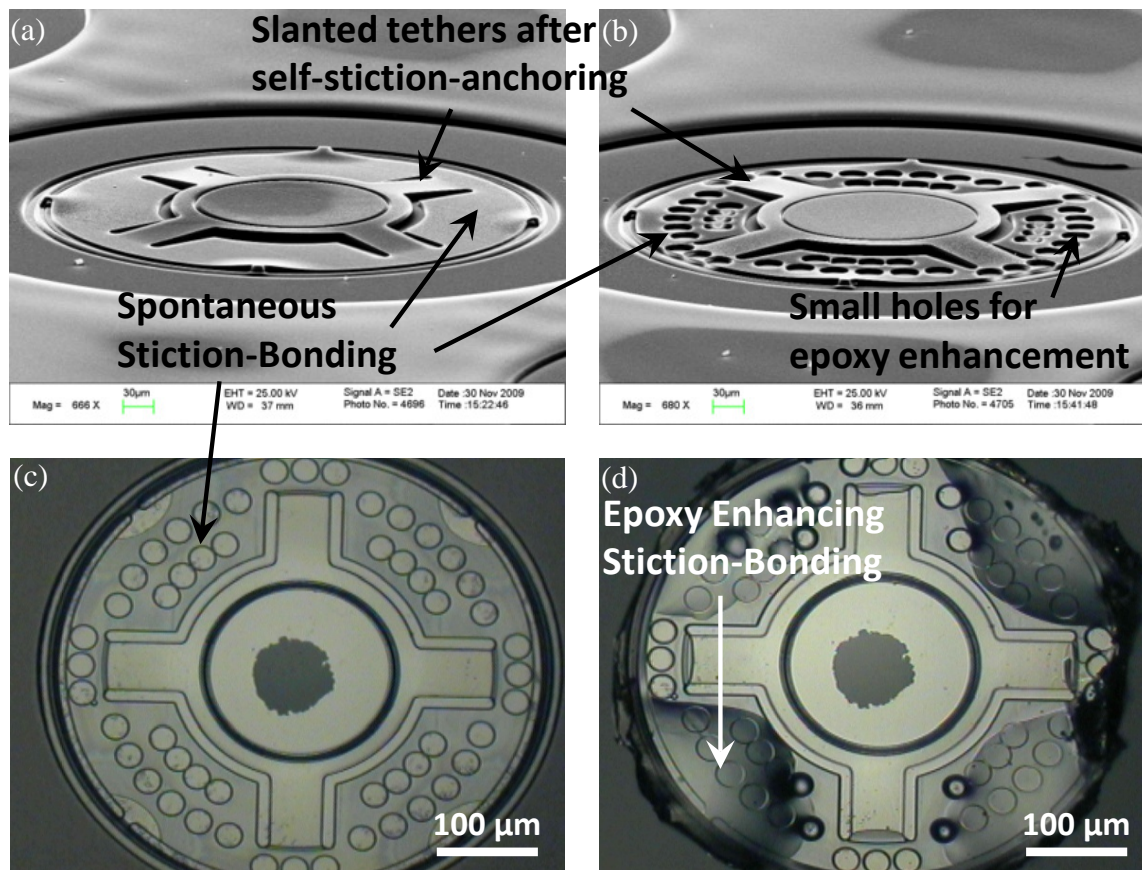


Figure 2-25: Fabrication results of the self-stiction-anchoring NC check-valves: (a) SEM picture showing the regular NC check-valve, (b) SEM picture showing the NC check-valve with small holes for epoxy enhancement, (c) top view of the NC check-valve, and (d) NC check-valve with epoxy bonding enhancement

2.6.3 Characterization of the self-stiction-bonding NC check-valve

To characterize the completed self-stiction-bonding NC check-valve, the same single check-valve packaging procedure as Figure 2-12 was adopted to accommodate

single NC check-valve in the capillary tube. On the other hand, the characterization setup represented in Figure 2-13 was also utilized to measure the NC check-valve's flow-rate profile. The pressure/flow-rate characteristic profile is shown in Figure 2-26. Liquid starts to flow at 0.2–0.3 psi (10–15 mmHg), and no obvious flow-rate is observed before the cracking pressure, showing that the sealing is well pressed by the four straight tether arms with the predetermined snapping force. This result meets our simulation expectation and provides the evidence that stiction does provide the required pre-stress force to create the cracking can secure the gap between the check-valve and the capillary tube opening.

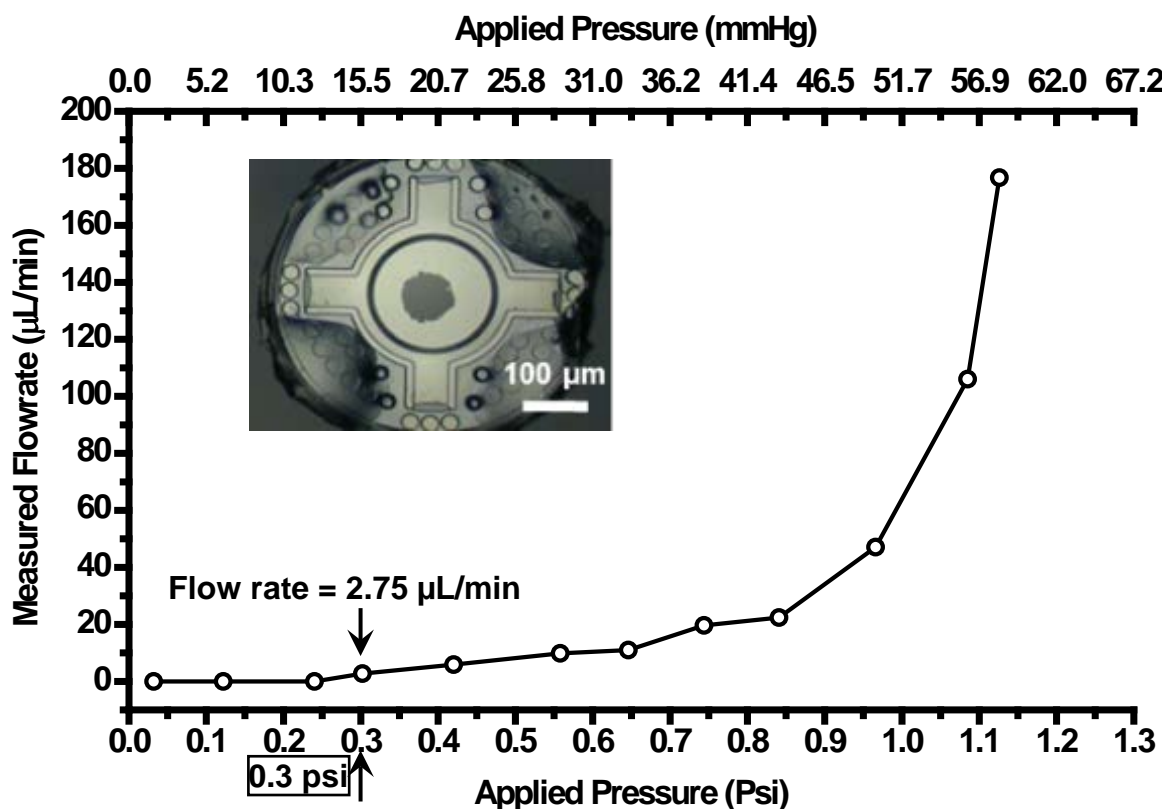


Figure 2-26: Pressure/flow-rate profile characterization results of the self-stiction-bonding NC check-valve

2.7 Blister Test of Stiction of Parylene-C Film

The self-stiction-bonding check-valve developed in Section 2.6 has demonstrated its successful regulating the microfluidic flow. However, since the cracking pressure of this check-valve is governed by stiction between the parylene-C film and the underlying substrate, a comprehensive study of stiction between parylene-C and different surfaces is required in order to understand, design, and create valves with specific cracking pressure and desired flow-rate profiles.

Stiction is an attraction that occurs between free standing micro-machined features and the substrate after the release of sacrificial photoresist [124]. Even though stiction is often an undesirable phenomenon, it can be employed to control the operation regime of thin film parylene-C check-valves. Attempts have been made to reduce stiction for specific check-valve geometries. For example, the cracking pressure of a polyimide check-valve with C_4F_8/Ar non-stiction coating changed from 210 kPa to 59 kPa [125], and SAM (self-assembled monolayer) is also used to reduce stiction [126].

The study in this section presents a comprehensive investigation of stiction between parylene-C and a variety of different surfaces using blister test. Blister test has been sophisticatedly used to measure the adhesion of two different materials and is capable to provide measurable results [127–137]. The surfaces under investigation include Au, Al, Si, parylene-C, XeF_2 treated Si, and silicon dioxide. After quantifying surface stiction, possible mechanisms that lead to stiction between parylene-C and various materials are explained. In addition, different recipes for sacrificial photoresist release that may affect the resulting stiction are also explored. Stiction results for different surfaces under different photoresist releasing methods show that surface coating

and releasing procedures used in this investigation can be used to control characteristics of parylene-C check-valves.

2.7.1 Experimental approaches

An outline of the fabrication procedure for stiction test devices is depicted in Figure 2-28. A backside circular trench 300 μm in diameter is created using DRIE until only a thin silicon membrane remains. Front side surface treatment is performed. These treatments include XeF_2 roughening, gold (0.2 μm) and aluminum (0.25 μm) deposition, parylene-C coating (2.5 μm), and silicon dioxide growth (1 μm). After surface treatment, sacrificial photoresist and 5 μm parylene-C layers are coated. Finally, DRIE is used again to remove the thin silicon film from the backside etching. Top views of the finished valves are shown in Figure 2-27.

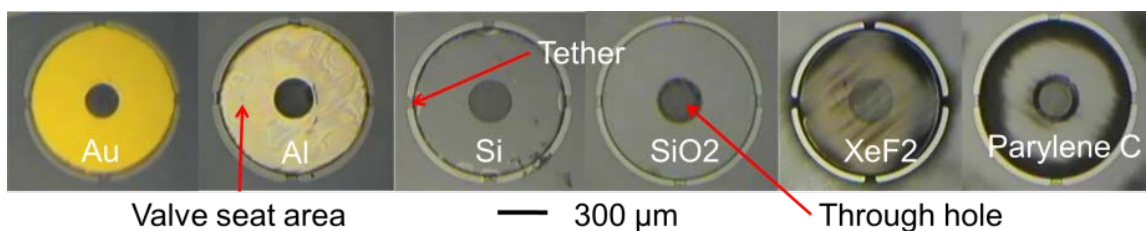


Figure 2-27: Top view of finished parylene-C check-valves fabricated for blister test

After dicing the wafer, different photoresist releasing methods are used. The sacrificial photoresist of all devices is released using ST-22, after which acetone is used to remove the ST-22 residue. Then, some valves are dipped in IPA (isopropyl-alcohol) and air dried. These valves are used for surface stiction characterization. Some valves are dipped in a mixture of acetone and 5 ml of silicone oil before air drying. These devices are used to study the effect of oil coating on parylene-C stiction. In addition, to

test the hypothesis of stiction mechanisms, some devices are subjected a 30 second HF (hydrofluoric acid) dip followed by a quick rinse in water to remove the acid. All devices are characterized using blister test.

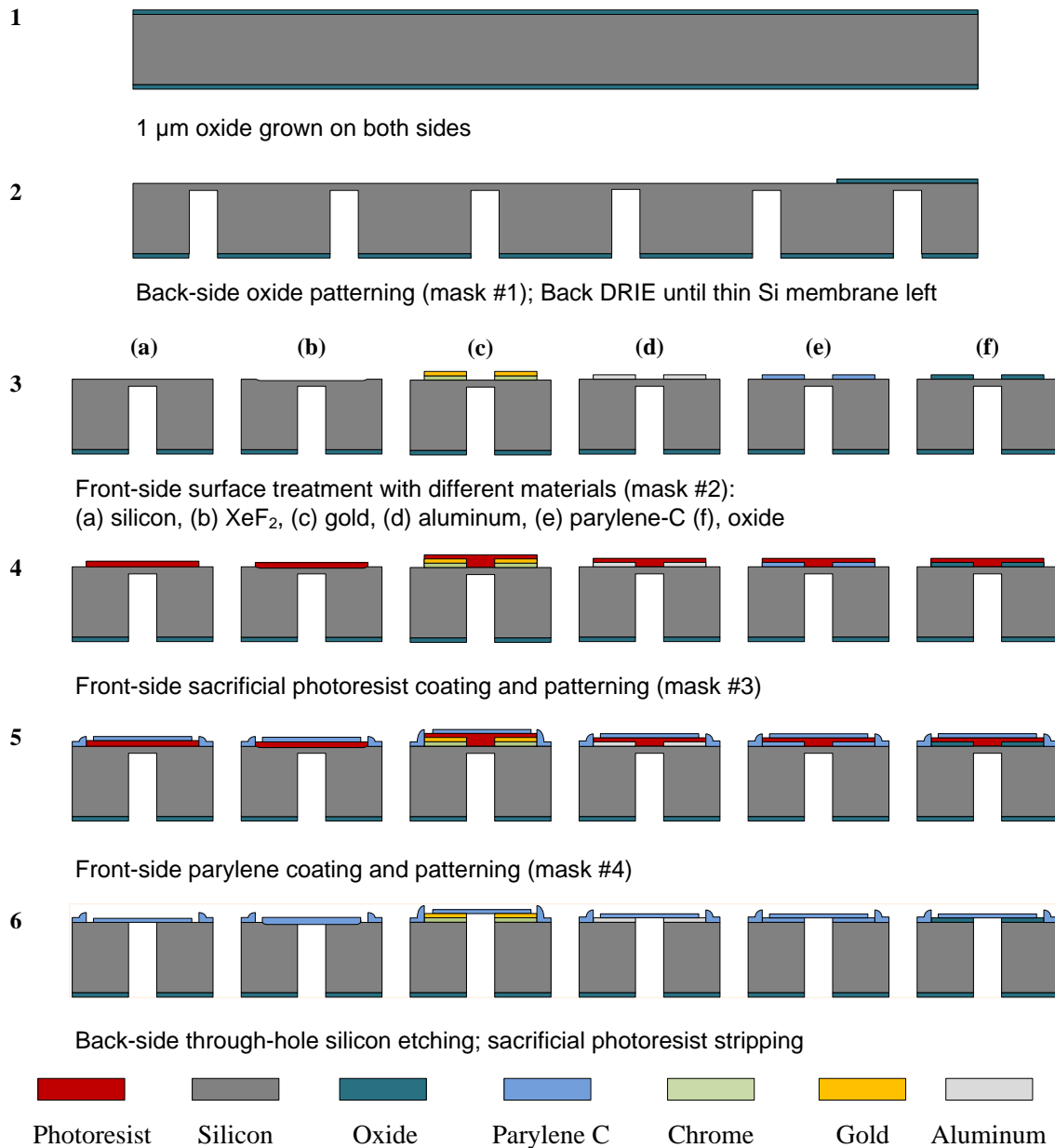


Figure 2-28: Fabrication procedures for circular parylene-C check-valve with different valve-seat surface treatments

2.7.2 Theory of blister test

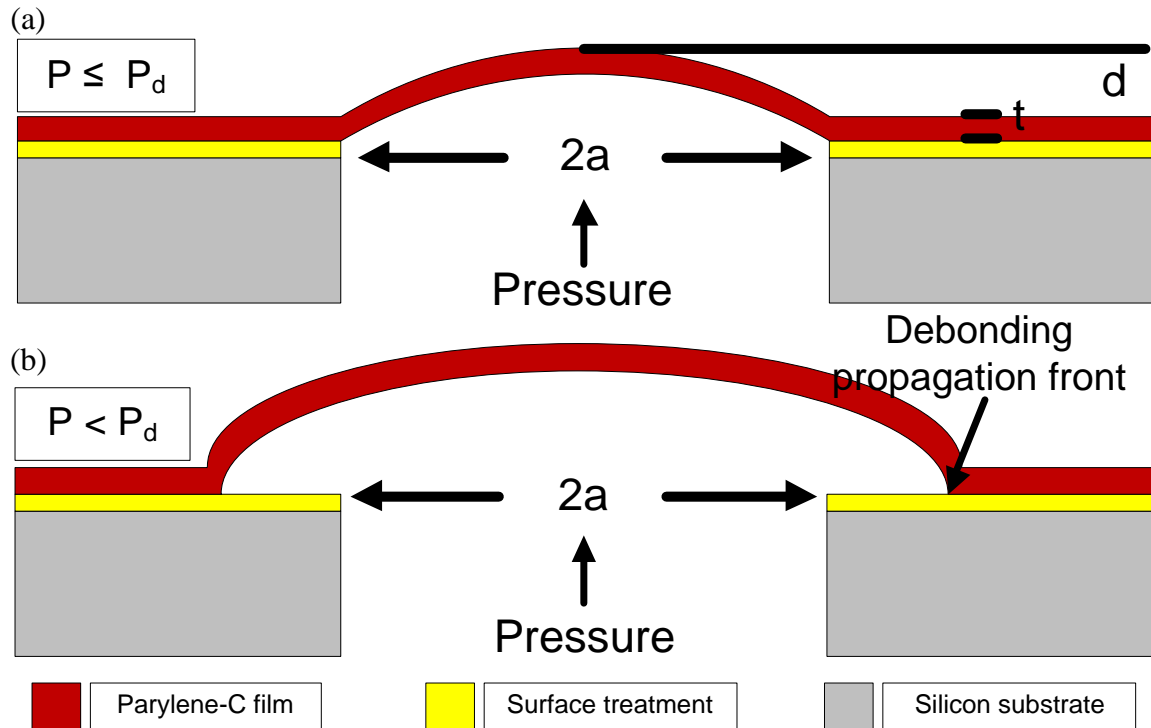


Figure 2-29: Theoretical blister formation during experimentation: (a) The applied pressure is less than or equal to the critical debonding pressure, P_c . (b) The applied pressure is higher than the critical debonding pressure, P_c ; the parylene-C film starts to propagate.

Blister test is usually performed on thin films overlying a solid substrate. Through holes are used to apply pressure to the film from the back side, as shown in Figure 2-29. When the applied pressure is less than the critical debonding pressure, p_d , the blister only buds up without any debonding. However, when the applied pressure is larger than p_d , parylene-C debonds from the silicon surface and propagate along the surface radially. For parylene-C check-valves, when pressure is applied, plastic deformation occurs in the parylene-C film that causes it to bulge to a distance d that is

dependent on the Young's modulus, E (~ 4 GPa), Poisson's ratio, ν (~ 0.4 [138]), geometry of the substrate opening, and thickness of the parylene-C film, t .

Due to the circular *via* in silicon, it can be assumed that the blister has a semispherical profile. With this assumption, the critical debonding pressure can be first calculated as [137]:

$$p_d = \frac{3.56Et}{a^4} d_c^3 + \frac{4\sigma_0 t}{a^2} d_c, \quad (2-23)$$

where d_c is the maximum vertical displacement of the parylene-C film, t is the thickness of the parylene film (3 μm in our experiment), a is the radius of the blister (100 μm). With the obtained critical debonding pressure, the stiction between parylene-C and silicon surface, γ , can be derived by

$$\gamma = 2.22Et \left(\frac{d_c}{a}\right)^4 + 2.00\sigma_0 t \left(\frac{d_c}{a}\right)^2, \quad (2-24)$$

where the constant σ_0 represents residual stress within the parylene-C film. For this particular experiment where parylene-C is annealed at 100°C, 37.8 MPa is used as the residual stress [138]. As the pressure inside the blister exceeds the critical pressure, p_d , parylene-C film debonds from the silicon surface and the obtained p_d from eqn. (2-24) is used to calculate the stiction, γ .

2.7.3 Blister test experimental setup

During experimentation, each die is placed in a testing jig that allows fluid (N_2 gas) to apply pressure to the parylene-C membrane. The jig is then connected to a fluidic setup consisting of a valve, a pressure regulator, and a pressure gauge, as shown in Figure 2-30. Figure 2-30 (a) shows the cross section view of the testing jig and Figure 2-30 (b) illustrates the overall view of the testing setup. The testing jig is placed under a

microscope for observation. Pressure inside the tubing is gradually increased by adjusting the pressure regulator. The pressure gauge reads out the current pressure inside the blister. The critical pressure is recorded when debonding occurs.

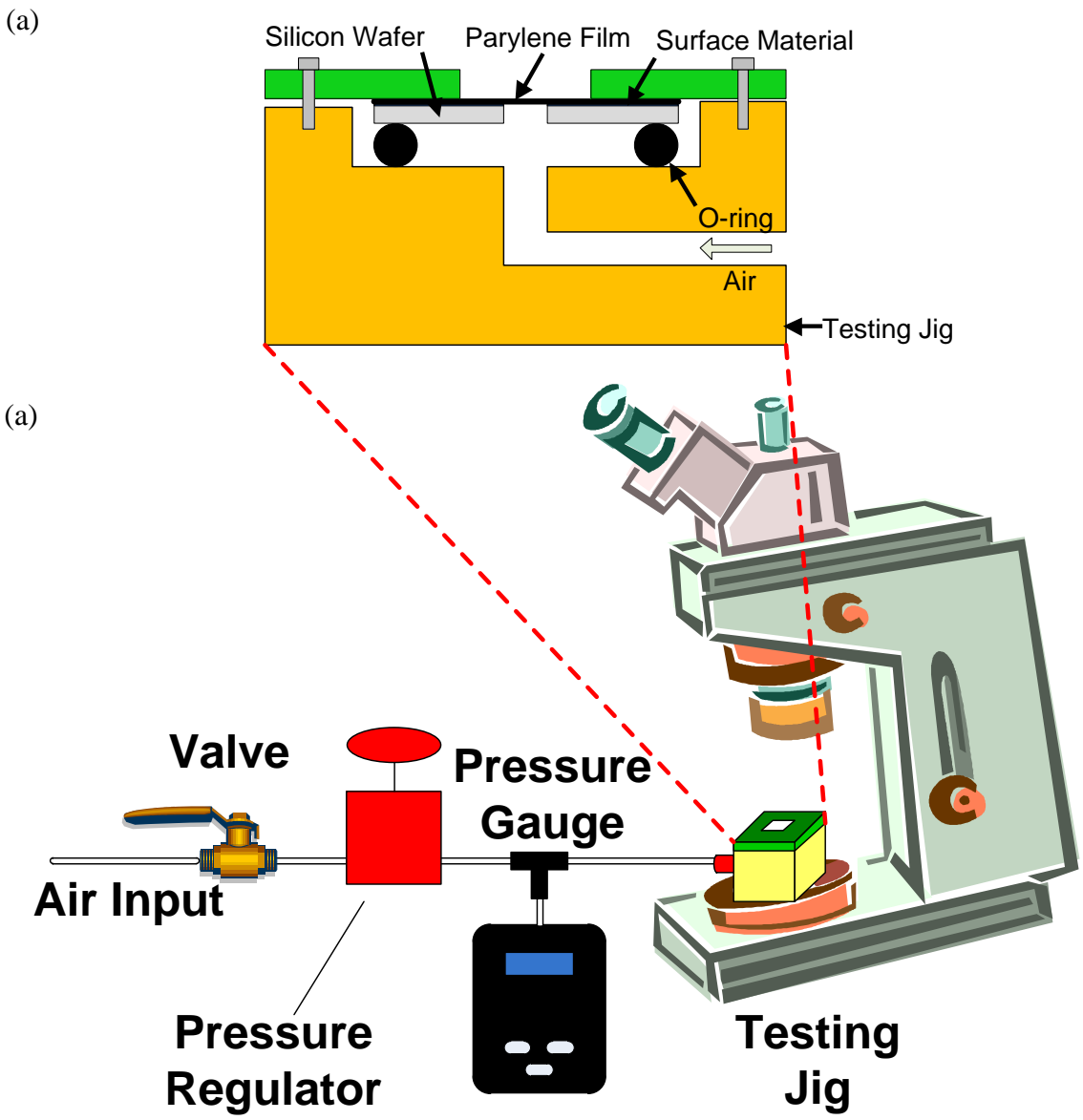


Figure 2-30: Experimental setup of the blister test: (a) the cross-section view of the test jig, and (b) schematic diagram of the testing setup

2.7.4 Testing results and discussion

A typical testing curve showing the relationship between the blister pressure and the passing time is shown in Figure 2-31. The parylene-C film starts to debond when the applied pressure is higher than the critical debonding pressure.

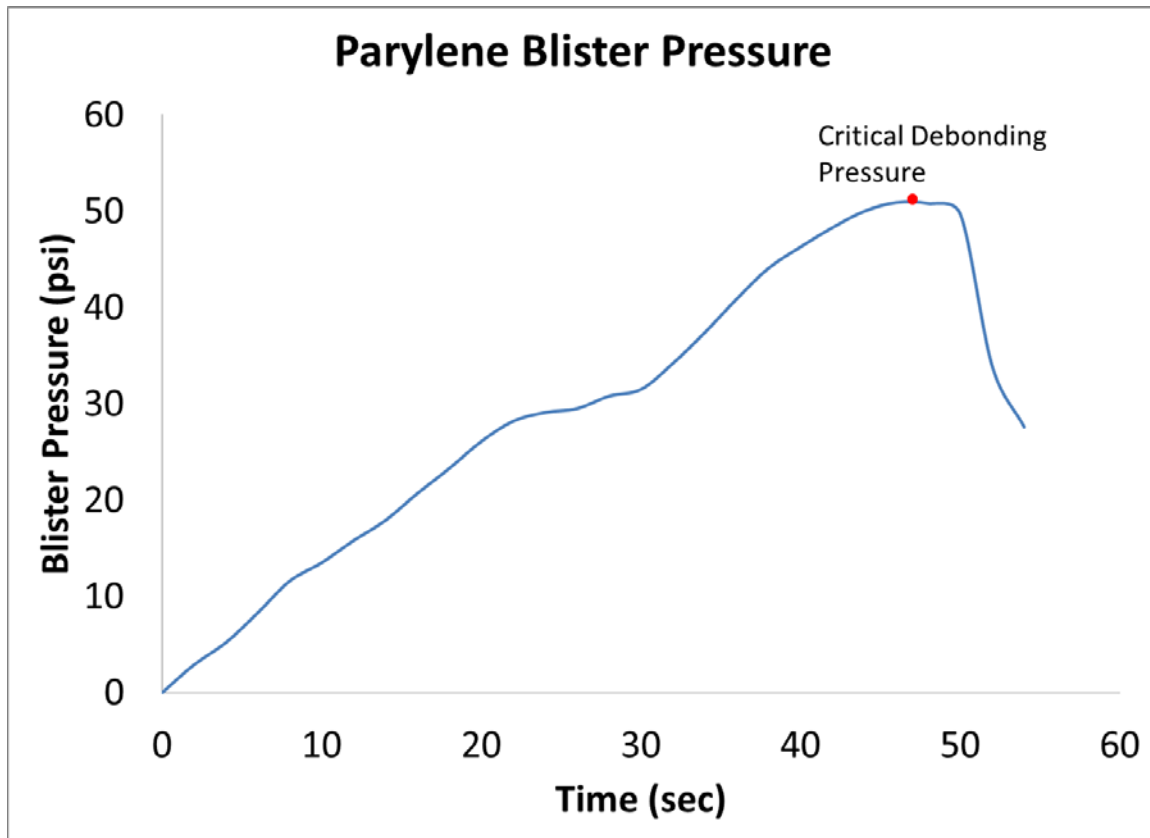


Figure 2-31: A typical curve of the blister test. The parylene-C film starts to debond when the applied pressure is higher than the critical debonding pressure.

Figure 2-32 illustrates the stiction between parylene-C and different surfaces after each device is soaked in acetone, IPA, and allowed to dry in air. In addition, the average cracking pressure of the valves is also recorded and listed in Table 2-2. The results show that Si has the greatest tendency to stick to parylene-C after drying (2.59 J/m^2). The high stiction of silicon to parylene-C can be explained by surface passivation. Even though

silicon and parylene-C are inherently hydrophobic, when they are subjected to water during photoresist release, the dangling bonds on the surface of the materials tend to bond to OH- groups in water. Such bonds make surfaces slightly hydrophilic. As the device dries, decreasing water content between the parylene-C film and silicon surface pulls the two surfaces together through hydrogen bonding, as illustrated in Figure 2-33. When the surfaces are extremely close from each other, Van der Waal's forces result in adhesion.

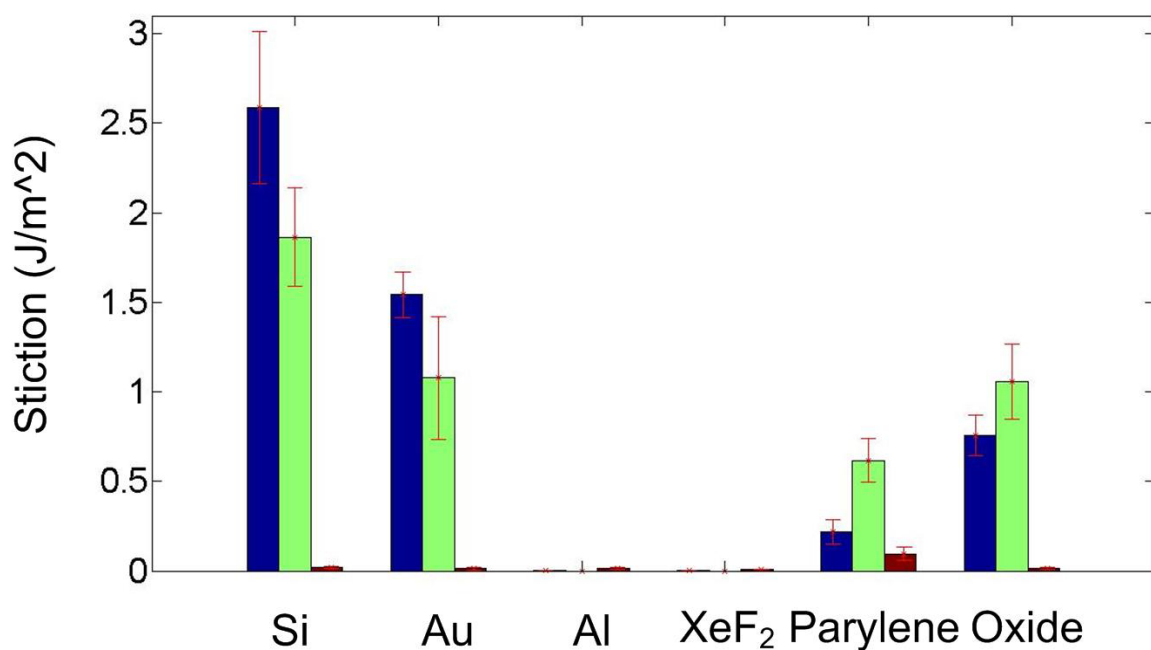


Figure 2-32: Stiction of parylene-C with different substrate surfaces after three kinds of releasing processes. Blue: acetone soak followed by IPA and water soak. Green: acetone soak followed by HF dip and water rinse. Red: soaking in mixture of acetone and silicone oil followed by direct air drying

Compared to Si, Au, oxide, and parylene all had gradually decreasing stiction to parylene-C. The decreasing values could be attributed either to increasing surface roughness or decreasing reactivity to OH- groups. Al and XeF₂ treated Si surfaces show almost no stiction to parylene-C. The former result can be attributed to the high surface

energy of aluminum, which precludes effective adhesion to most materials. On the other hand, XeF₂ treated Si surface display huge surface roughness. As a result, very little silicon surface actually come into contact with parylene-C. Thus, Van der Waal's force is not great enough to cause significant stiction.

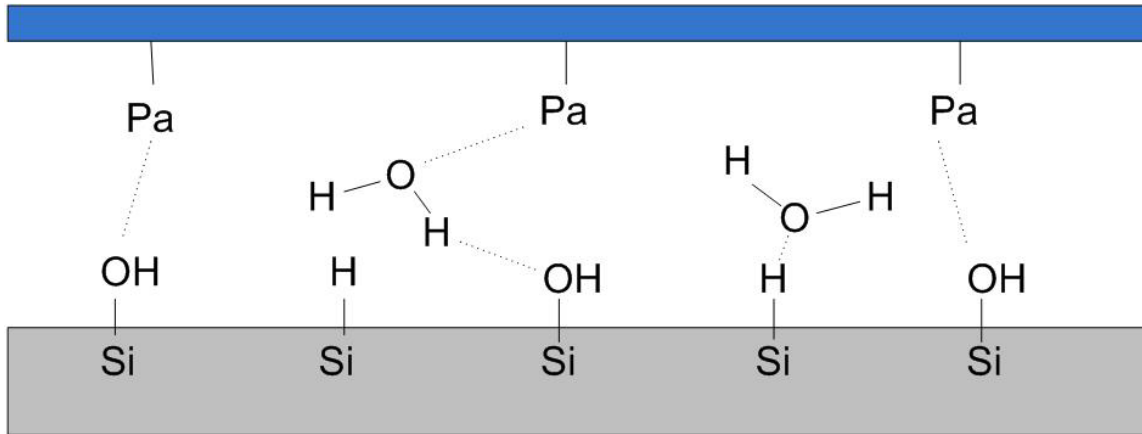


Figure 2-33: Hydrogen bonding that occurs between water molecules and the passivated silicon surface. As the device dries, decreasing water content between the parylene-C film and the silicon pulls the two surfaces together through hydrogen bonding.

Table 2-2: Cracking pressure of parylene check-valves under different releasing procedures: (1) acetone and IPA soak followed by air drying, (2) HF dip, water rinse, followed by air drying, (3) soak in a mixture of acetone and silicone oil before air drying. Zero stiction means that the stiction is too small to be measured effectively.

Release method	1 (J/m ²)	2 (J/m ²)	3 (mJ/m ²)
Si	2.59	1.86	18.5
Au	1.54	1.07	12.5
Al	0	0	13.2
XeF₂	0	0	8.2
Parylene	0.22	0.62	95.6
Oxide	0.76	1.06	13.9

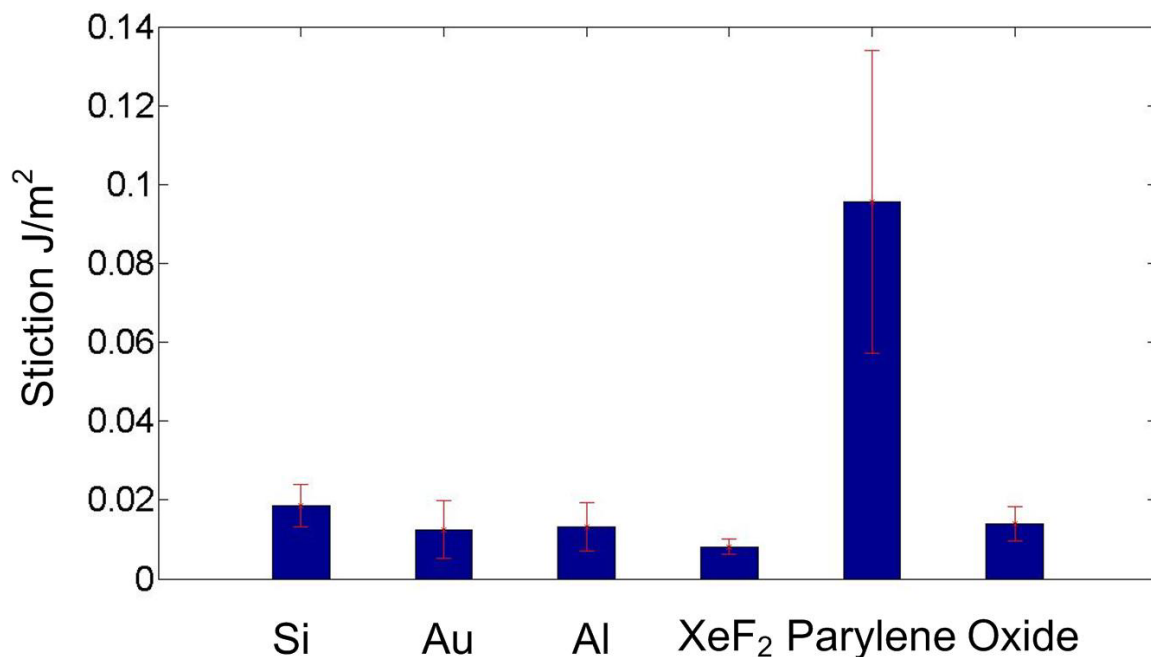


Figure 2-34: Stiction between parylene-C and various surfaces after releasing in a mixture of acetone and silicone oil

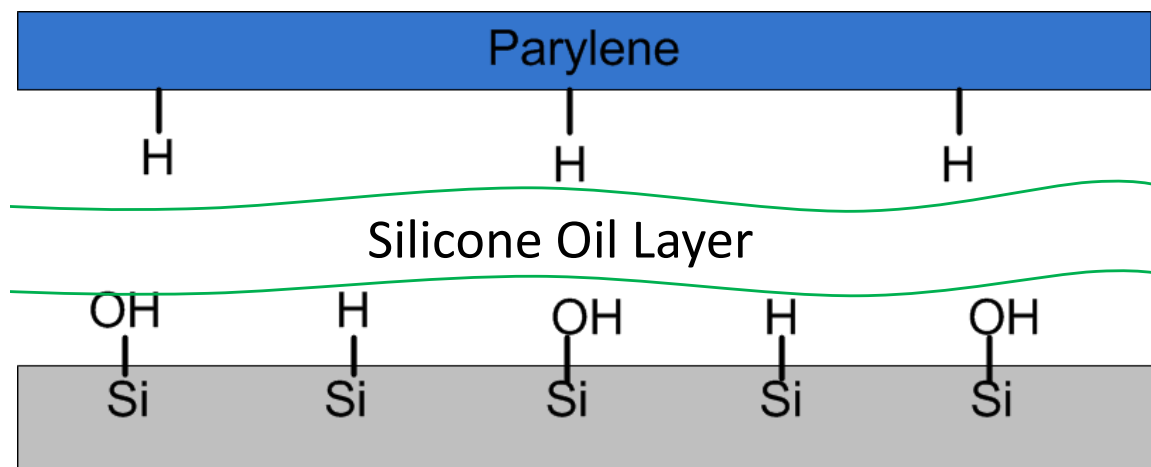


Figure 2-35: Stiction between the parylene-C and the silicon surface is reduced due to the silicone oil layer, which reduces surface passivation and the proximity between surfaces.

Following the second photoresist releasing method where devices are air dried after soaking in a mixture of acetone and silicone oil, stiction between parylene-C and all

surfaces are reduced, as shown in Figure 2-34. Results show that, other than parylene-C, all stiction values are between 0.01 and 0.02 J/m². These results suggest that, after silicone oil coating, stiction is no longer caused by the interaction between parylene-C and substrate surfaces but by the adhesion between parylene-C and the oil layer. Since this oil layer reduces surface passivation and the proximity between surfaces, stiction is decreased, as shown in Figure 2-35. The relatively high stiction value between two parylene-C surfaces can be explained by the roughness of the parylene surface, which increases its effective area to interact with silicone oil.

In order to verify the proposition that surface passivation contributes to stiction, some devices are subjected to a short HF dip before drying. This HF dip should remove some surface –OH bonds and thus reduce stiction. Results from blister tests done on these valves reveal that for certain material surfaces (i.e., Si and Au), HF dip does decrease stiction slightly, as shown in Figure 2-32. Even though HF dip removes much of the hydroxyl groups, the ensuing rinse in water probably introduces some –OH groups back. As a result, stiction still remains.

2.7.5 Summary

This study successfully quantifies stiction between thin film parylene-C and various surfaces. Devices with valve configurations were fabricated and released using various procedures. After performing blister tests, stiction values were recorded. The mechanisms that lead to stiction or the reductions thereof include surface passivation with hydroxyl groups, surface roughness, and surface proximity. Experiments show that mechanisms that can reduce the proximity between parylene-C and other surfaces during drying will likely reduce stiction. In addition, since different surface treatments result in

different stiction, all processes and photoresist releasing methods from this study can be used to design parylene-C check-valves with different cracking pressures.

2.8 Summary and Conclusion

2.8.1 Comparison of different types of micro check-valves

In this chapter, a parylene-C-based NC check-valve paradigm was proposed and developed. The standard NC check-valve structure consists of slanted parylene-C tethers with built-in residual tensile stress. These pre-stressed slanted parylene-C tethers provide the necessary downward force, giving the desired cracking pressure of the NC check-valve.

Three different methods were developed to create the slanted tethers. The first method adopted the gray-scale photolithography to generate the sloped sacrificial photoresist as the mold of the following deposited parylene-C film. The second approach utilized the post-fabricated pop-up structural design to generate the desired slanted tethers. The third method adopted the stiction phenomenon that inevitably takes place after the drying process to create the slanted slope created using height differences of the parylene-C structure. The residual stress built in the parylene-C tethers can be achieved by stretching the tether, thermal annealing and quenching afterward, or combination of both. The cracking pressure can be manipulated by several parameters such as the number of the slanted tethers, the sloping angle of the slanted tethers, the geometry of the slanted tethers (the width and the thickness), and also the residual stress of the slanted tethers which can be controlled by the annealing temperatures. Table 2-3 shows the comparison of all different check-valves introduced in this chapter. It can be seen that thermal annealing are capable of providing the highest cracking pressure (2.9 psi) among

the three kinds of slanted tether NC check-valves. Therefore, NC check-valves pre-stressed by thermal annealing is suitable for high-pressure applications. In addition, to obtain even higher cracking pressure system, multiple NC check-valves can be integrated in series to meet the request of the extremely high cracking pressure applications. The characterization results demonstrated the additivity property of the integration of multi NC check-valve's cracking pressure. On the other hand, NC check-valves pre-stressed only through pop-up mechanism or self-stiction bonding mechanism are appropriate for the applications where low cracking pressure usage is needed.

Table 2-3: Comparison of different slanted tether parylene-C NC check-valves introduced in this chapter. Water was used as the working fluid.

Check-valve type	NC	NC	NC	Integration of multiple NC in series
Creation of slanted tethers	Gray-scale lithography	Post-fabrication pop-up	Self-stiction bonding	---
Cracking pressure (psi)	0.3–2.9	0.35	0.3	2.06 (Combining for four NC check-valves)
Breakdown pressure (psi)	> 25	> 25	> 25	> 25

In addition, a study of parylene-C stiction to several different kinds of surfaces was performed by utilizing the blister test in this chapter as well. Experimental results showed that the stiction strength of parylene-C to other surfaces would be influenced by the surface with hydroxyl groups, surface roughness, and surface proximity.

2.8.2 Lifetime of the slanted tether NC check-valves

Because parylene-C served as the main structural material of the NC check-valves developed here, it begs the question of how long the residual tensile stress would last within the parylene-C tethers. The question is actually related to the viscoelastic/viscoplastic properties of parylene-C, which has rarely been explored in the past. Therefore, the creep and stress relaxation behavior and other types of viscoelastic/viscoplastic properties of the parylene-C will be discussed at length in chapter 5.

